BOLT BERANEK AND NEWMAN INC

CONSULTING • DEVELOPMENT • RESEARCH

Report No. 1532
Job No. 11244

ON THE OPTIMAL BEHAVIOR OF THE HUMAN CONTROLLER: A PILOT STUDY COMPARING THE HUMAN CONTROLLER WITH OPTIMAL CONTROL MODELS

Contract No. NAS12-104

Jerry D. Burchfiel
Jerome I. Elkind
Duncan C. Miller

15 August 1967

Submitted to:

National Aeronautics and Space Administration
Control and Information Systems Laboratory
Electronics Research Center
575 Technology Square
Cambridge, Massachusetts 02139

Attention: Mr. William A. Wolovich

Report No. 1532

BBN Job No. 11244

ON THE OPTIMAL BEHAVIOR OF THE HUMAN CONTROLLER: A PILOT STUDY COMPARING THE HUMAN CONTROLLER WITH OPTIMAL CONTROL MODELS

Jerry D. Burchfiel
Jerome I. Elkind
Duncan C. Miller

15 August 1967

Prepared under Contract No. NAS12-104 by
Bolt Beranek and Newman Inc
Cambridge, Massachusetts

for

Control and Information Systems Laboratory
NATIONAL AERONAUTICS AND SPACE ADMINISTRATION
Electronics Research Center
575 Technology Square
Cambridge, Massachusetts 02139

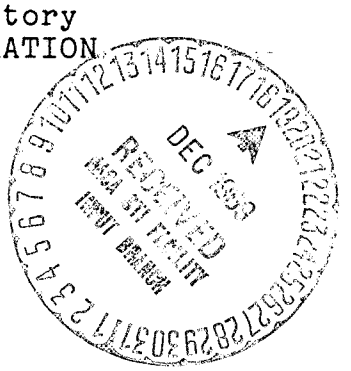

ABSTRACT

It is postulated that the human controller acts in a near optimal manner given his inherent structural constraints. These constraints are approximated by a time delay. The optimal controller for a linear plant with a quadratic cost functional which takes into account this time delay limitation is derived. The optimal controller contains a model of the plant being controlled plus linear dynamics operating on the difference between the output of the real plant and that of the model. A pilot experiment was performed to test the hypothesis that the human controller is nearly optimal. Good agreement between human and optimal controller behavior was obtained. The differences between the two behaviors can be accounted for by assuming a subjective cost functional that the human controller attempts to optimize.

TABLE OF CONTENTS

LIST OF ILLUSTRATIONS

CHAPTER I

INTRODUCTION

The human controller of dynamic systems is a self adaptive controller. If he is told the objective of a control task and the extent to which he has achieved this objective, he will through training or practice attempt to improve his performance, provided he is motivated to do so. It is reasonable, therefore, to assume that a highly-trained human controller will act in a near optimal manner, subject to certain internal constraints that limit the range of his behavior and also to the extent to which he understands the objective of the control task.

Given the self-optimizing tendency of the human controller it is productive to look to optimal control theory as a source of, and an inspiration for models of human controller behavior. During the late 1940's and early 1950's attempts were made by Phillips (Ref. 1) and Elkind (Ref. 2) and others, to use Wiener (Ref. 3) optimization theory as a basis for models of the human controller and for predicting human behavior. More recently, with the development of modern optimal control theory, (Ref. 4 and 5) there has been a resurgence of interest in optimal control models for the human controller. Roig (Ref. 6) and Leonard (Ref. 7) compared the mean-squared error performance of the human operator with that of various optimal controllers and found that the human controller tended to behave in a near optimal manner. Obermeyer and Muckler (Ref. 8) examined existing manual control data and attempted to

solve the inverse problem, that is, to find the cost functional that the human controller minimized in these manual control situations. In a later study Obermeyer, Webster and Muckler (Ref. 9) investigated the effects of performance criteria on compensatory rate control tracking. In a pilot study performed by one of us, Miller (Ref. 10), the effects of changes in the cost functional upon tracking performance was demonstrated.

The results of these earlier studies indicate that it is reasonable to postulate that the human controller tends to behave in a near optimal manner and that optimal control theory provides an appropriate theoretical framework for understanding human controller behavior. To test this theory, however, it is necessary to use procedures somewhat different from those normally employed in the more conventional experimental studies of human controller characteristics. The experimental situation must be constructed so that it is consistent with the theory. In particular, the input disturbances if noise-like, should be derived by passing white noise through (preferably) low-order linear filters. The cost functional must be explicitly defined by the experimenter and communicated in a meaningful way to the subject. Constraints and invariances in the human controller's characteristics must be identified. Finally, the optimal controller, the one that will minimize the cost functional subject to these constraints, must be derived.

Most of the experiments that were performed to develop and test conventional control models for the human controller were not designed with these constraints in mind. As a result it is difficult to use the results obtained from them to test hypotheses about the optimality of the human controller and the reasons for his deviations from optimum. As we begin to understand more about the optimal behavior of the human controller, it is likely to be

possible to use this large body of earlier data, but for the present it is necessary to perform additional new experiments specifically designed to probe the question of human controller optimality.

In this report we discuss the first of a series of experiments on the application of optimal control theory to manual control systems. In this present study we have investigated, within the context of a very simple control situation, the extent to which an optimal control model represents human controller behavior when the cost functional is a weighted sum of mean-squared error and mean-squared control action. The principal independent parameter of this experiment was the relative weighting of mean-squared error and mean-squared control action. As the first step in the application of optimal theory to this experimental situation we derive the optimal controller under the assumption that the input disturbance is integrated white noise and that the human controller's characteristics include a time delay. The optimal controller structure that we developed has an internal model for the plant being controlled, an optimal estimator (predictor) of the state of the plant which compensates for the time delay, and a simple amnesic controller operating on the estimated state. The derivation of the controller is discussed in Chapter II in which we consider the general problem of an n^{th} order plant and then specialize it to the first-order plant that was investigated experimentally.

In Chapter III we describe a pilot experiment that was performed to test the optimality of the human controller and the effects of relative weighting of control and error on his performance. In Chapter IV we present and discuss the results of these experiments.

An important factor introduced in this discussion is the concept of the subjective cost functional and we show how the introduction of a subjective relative weighting accounts for most of the difference between optimal and human controller behavior.

CHAPTER II

DERIVATION OF THE OPTIMAL CONTROL MODEL FOR THE HUMAN CONTROLLER

A. INTRODUCTION

We have postulated that, subject to certain constraints, the human acts as a near optimal controller. In this chapter we derive the optimal control law for the system we have investigated experimentally. This system was a linear, first-order plant perturbed by filtered white gaussian noise as shown in Fig. 1. The human controller's task was to act as a state regulator and to minimize a cost functional which was the weighted sum of two terms: a quadratic function of the state, and of the control action. The relative weighting of these two terms was a parameter of the experiments.

We have assumed that the principal constraint on the human controller's characteristics is a time delay, e^{-sT}. This delay takes account of the controller's processing time and also approximates the characteristics of the neuromuscular system. We derive the optimal control law for filtered white gaussian disturbances for a controller containing such a time delay. We use these results to predict the human controller's characteristics and, in particular, to predict how his characteristics will depend upon the relative weighting in the cost functional of the control action.

B. OPTIMAL CONTROL OF A LINEAR SYSTEM WITH QUADRATIC COST CRITERIA

Given a linear system described by the vector differential equation

$$\dot{x} = Ax + Bu \tag{1}$$

where x is the state and u the control, and a cost functional

$$J = \frac{1}{2}\int_0^\infty [x'Qx + u'Ru]dt, (R>0,\ Q\geq 0) \tag{2}$$

we wish to find the optimal control u(t) which minimizes J subject to the initial condition $x(0) = x_o$.

It is shown in Ref. 4 that the optimal control for this situation is

$$u^*(t) = -R^{-1}B'K \tag{3}$$

where K is the symmetric positive definite solution of the Matrix Riccati Equation:

$$0 = KA + A'K + Q - KBR^{-1}B'K \tag{4}$$

The closed-loop (optimally controlled) system will now obey the differential equation:

$$\dot{x} = (A - BR^{-1}B'K)x,\ x(0) = x_o \tag{5}$$

so the optimal trajectory is

$$x^*(t) = e^{(A-BR^{-1}K)t} x_o \quad \text{for } t>\emptyset$$

and (6)

$$u^*(t) = R^{-1}B'Ke^{(A-BR^{-1}B'K)t} x_o \text{ for } t > 0$$

It is also shown in Ref. 4 that the total cost, starting from initial displacement x_o, is

$$J(x_o) = \frac{1}{2} x_o'Kx_o \; . \tag{7}$$

C. CONTROL OF A LINEAR SYSTEM WITH TIME DELAY

1. Deterministic Case: Initial Disturbance.

We now wish to investigate the system shown in Fig. 1: a linear plant followed by a time delay of T sec.

The dynamics are again

$$\dot{x}(t) = Ax + Bu \; ; \; x(0) = x_o \tag{8}$$

and the cost is

$$J = \frac{1}{2} \int_o^\infty [u'Ru + x'Qx]dt, \text{ with } R>0 \text{ and } Q \geq 0 . \tag{9}$$

Now, however, only a delayed version of the state of the plant integrators ($x_d(t) = x(t-T)$) is available as input information to the controller. The cost functional may be expressed in an

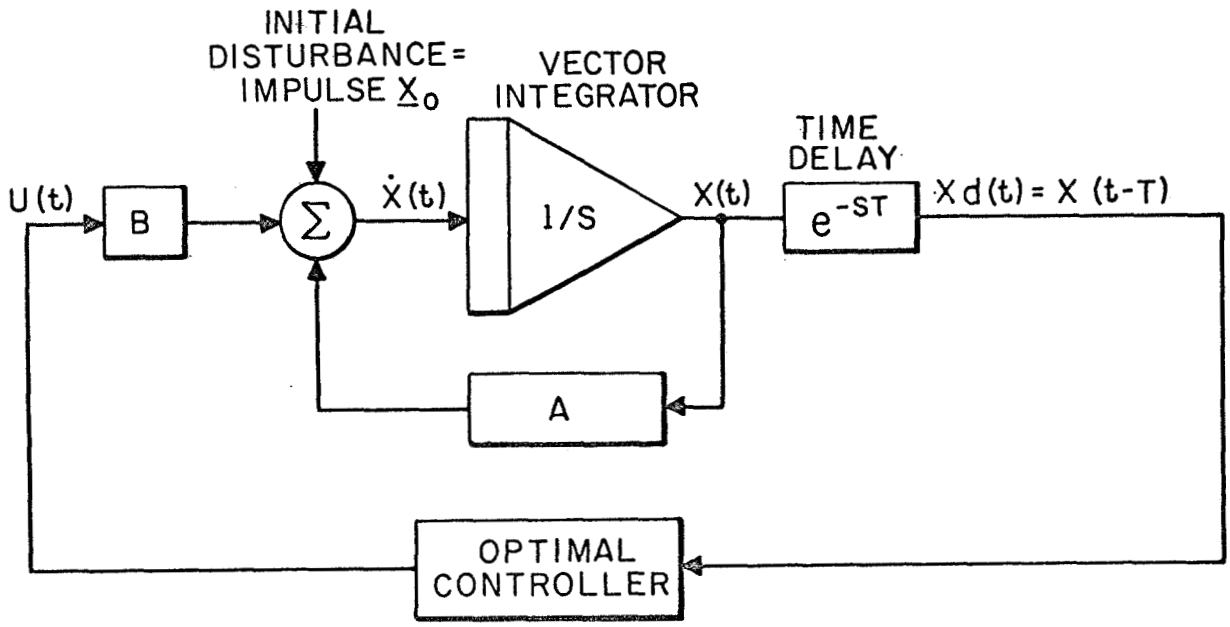

FIG.1 CONTROL PROBLEM WITH TIME DELAY

alternate form by a change in variables in the second term of the integrand; $\tau = t-T$:

$$J = \frac{1}{2}\int_0^\infty [u'Ru + x'_d Q\, x_d]d\tau \qquad (10)$$

This form is equivalent to Eq. (9) because we assume that the system is initially at rest, i. e., for $t<0$ the state $x(t)$ and the control $u(t)$ are uniformly zero. This implies that the output of the time delay, $x_d(t)$, will be uniformly zero for $t<T$, then take a step to x_o at $t=T$. ($T\geq 0$)

We place two important constraints on the optimal feedback controller: first, that at time T it has only the information $x_d(t)$, $t\leq T$, available to develop a control strategy; in particular, it does not have available the present state of the integrators, $x(T)$ merely their state T seconds ago: $x_d(T) = x(T-T)$. The second constraint we place on the controller is that it be realizable, i.e., that it cannot respond to an input before that input occurs.

These two constraints insure that the control response $u(t)$ will be uniformly zero for $t<T$. (Since $x_d(t) \equiv 0$ for $t<T$).

At time T, x_d takes a step such that $x_d(T) = x_o$. This is sufficient to specify (to whatever strategy is inside the controller) that the initial disturbance at $t=0$ was a vector impulse having value x_o. Further, $u(t)$ was uniformly zero for $t<T$, there were no other inputs to the system, and (by assumption) the state of the system at $t=0_-$ ($x(t), -T\leq t<0$) was zero.

This yields the result that $x(t) = e^{At}\, x_o$ for $0\leq t<T$. This is enough to specify the entire state of the plant at $t=T$. The

optimal controller now only needs to find the optimal control $u^*(t)$, $t>T$, based on this perfect knowledge of the state of the system at $t=T$.

The cost may thus be expressed as

$$J' = \frac{1}{2}\int_T^\infty [u'Ru + x'Q\,x]dt \tag{11}$$

since $u(t)$ and $x(t)$, $t<T$ are completely independent of the control strategy to be selected. A shift in variables ($\tau=t-T$) makes this problem identical (except for an initial condition) to that discussed in the previous section (which had no time delay in the plant). The differential equations:

$$\dot{x}(\tau) = Ax(\tau) + Bu(\tau)\ ;\ x(0) = e^{AT}\,x_o \tag{12}$$

and

$$J = \frac{1}{2}\int_o^\infty [u'Ru + x'Qx]d\tau. \tag{13}$$

The optimal control $u^*(\tau)$ will thus be of the same form as the previous solution:

$$u^*(\tau) = -R^{-1}B'Ke^{(A-BR^{-1}B'K)\tau}e^{AT}\,x_o \text{ for } \tau > 0 \tag{14}$$

where K is again the positive definite solution of

$$0 = KA + A'K + Q - KBR^{-1}B'K,$$

and

$$u^*(t) = \begin{cases} 0 \text{ for } t<T \\ -R^{-1}B'Ke^{(A-BR^{-1}B'K)(t-T)}e^{AT}\,x_o \text{ for } t\geq T \end{cases} \tag{15}$$

Given this optimal control input, we can solve for x(t), t>T, by convolution. The result is:

$$x^*(t) = \begin{cases} 0 \text{ for } t<0 \\ e^{At} x_o \text{ for } 0 \leq t < T \\ e^{(A-BR^{-1}B'K)(t-T)} e^{AT} x_o \text{ for } t \geq T \end{cases} \quad (16)$$

These responses are shown schematically in Fig. 2.

At this point, the optimal controller is specified (nonuniquely) by its input-output characteristic. In particular its output is $u^*(t)$ (shown in Fig. 2) whenever its input is $x_d^*(t)$ (also shown in Fig. 2).

Two generalizations are possible at this point: first, since the derivations above and in Ref. 5 hold true for <u>any</u> x_o, and the input and output of the controller are each linear in x_o, then the desired transfer function from $x_d(t)$ to $u(t)$ can be realized by a linear system whose parameters are <u>independent</u> of x_o.

Second, the plant is time-invariant; if the initial disturbance occurs at t_o rather than t=0, (with the state of the plant being uniformly zero for $t<t_o$), then a change of variables results in our original optimization problem: the optimal responses shown in Fig. 2 are merely shifted in time by t_o. This means that the optimal feedback can be realized by a time-invariant system.

It is, of course, not necessary to use a linear time-invariant system to realize the optimal feedback controller; the same transfer could be obtained from any of an infinite number of nonlinear time-varying systems. However, as long as the controller

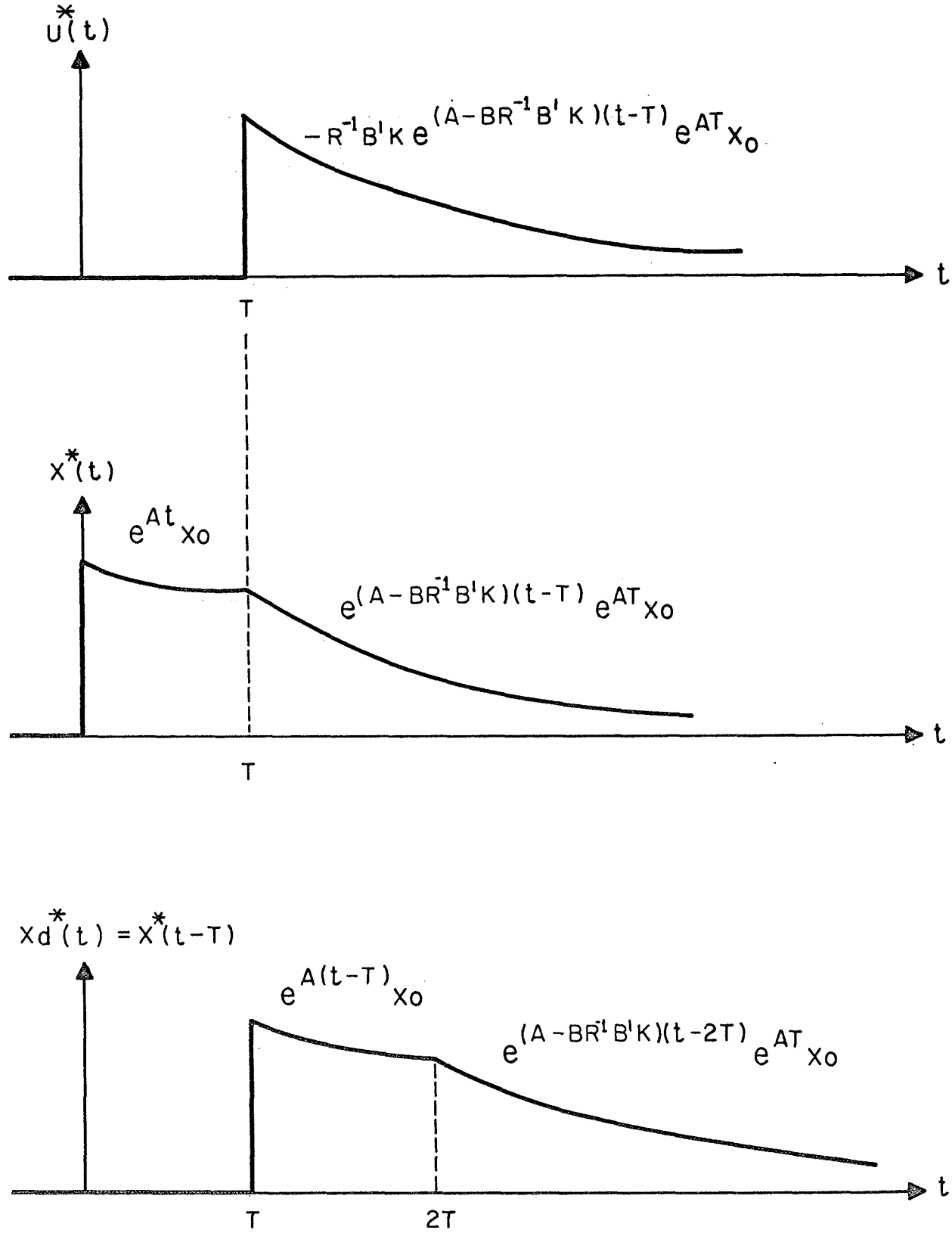

FIG. 2 REPRESENTATIVE RESPONSES OF OPTIMALLY CONTROLLED PLANT WITH TIME DELAY

is realizable and at t=T has only knowledge of $x_d(t), t \leq T$, then none of these more complicated controllers can yield a cost J lower than that provided by a linear time-invariant feedback controller. For this reason, we will investigate only controller realizations in the class of linear, time-invariant systems.

One such realization is shown in Fig. 3. This controller structure contains an exact model of the plant to be controlled, including the time delay, and is driven by the same input u(t). The state of the integrators and the observable output of this model are denoted as $\tilde{x}(t)$ and $\tilde{x}_d(t)$, respectively. A signal representing the observed difference in the behavior of the plant and the model of the plant is denoted by $i(t) = x_d(t) - \tilde{x}_d(t)$. This difference between observed and predicted behavior is operated on by a finite dimensional linear time-invariant dynamical system (a N-input, N-output lead-lag network) to develop the estimate of the present state of the plant integrators, $\hat{x}(t)$, to provide $u^*(t)$. All initial conditions in the controller, both in the model and in the finite-dimensional linear system, are uniformly zero, i. e. the controller state is uniformly zero, for t<T.

Note that this process of optimal control may be viewed as two completely separate subprocesses: the first of these is the estimation process, which develops an estimate, $\hat{x}$, of the present state of the plant integrators, x, by operating on the difference between observed and predicted plant behavior. The second process is control, developing the optimal control for the plant by matrix gain operation on the estimate $\hat{x}(t)$. In fact, this matrix gain is exactly the gain which yields the optimal control from the true state of the plant when there is no time delay.

The behavior of the four quantities x(t), $x_d(t)$, i(t) and $\hat{x}(t)$ is shown schematically in Fig. 4. We note that the estimator $\hat{x}(t)$

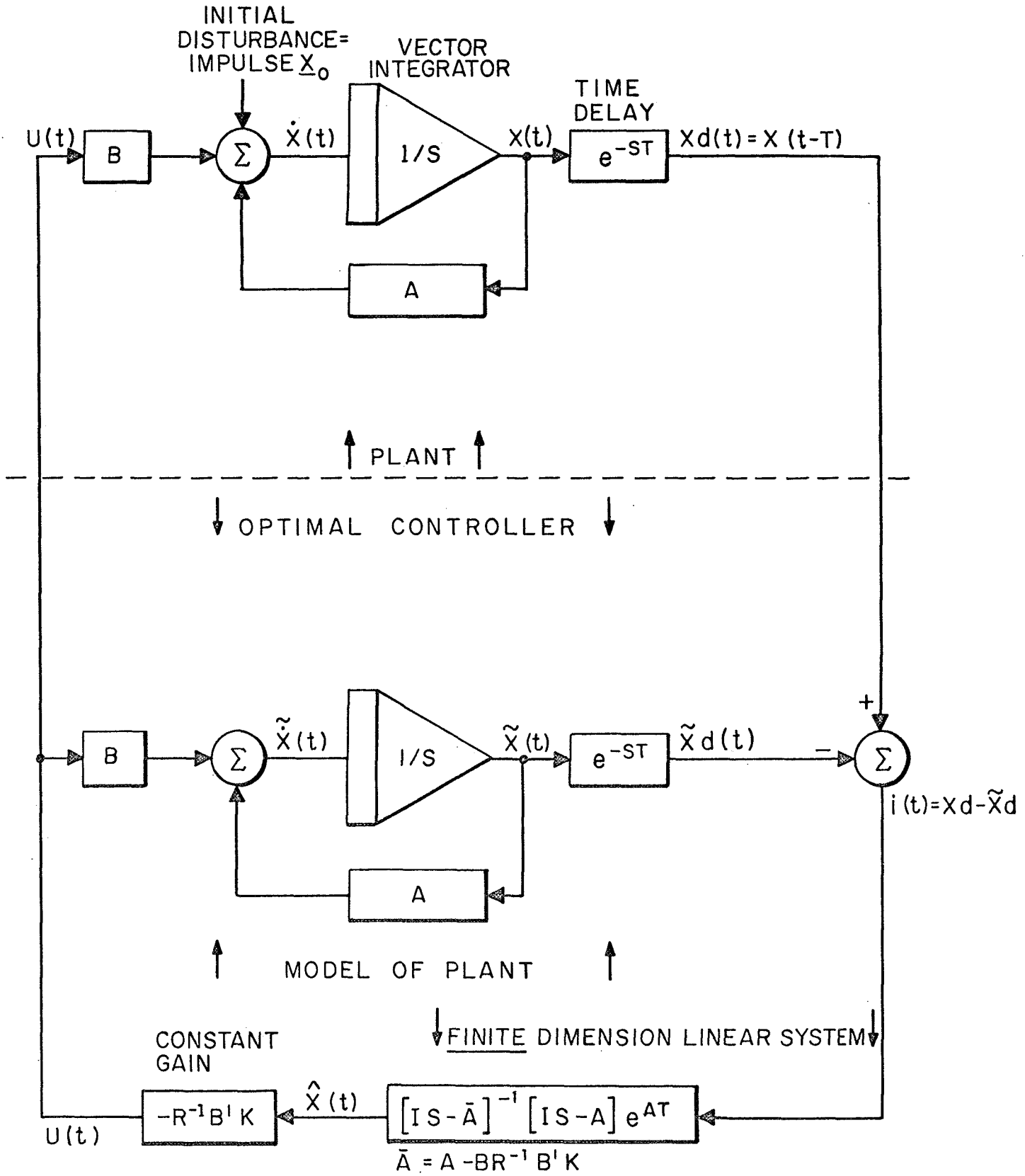

FIG. 3 A REALIZATION OF THE OPTIMAL CONTROLLER

remains zero for $t<T$, but for $t>T$ follows the state exactly where

$$x(t) = e^{\bar{A}(t-T)}x_o \quad (\bar{A} = A-BR^{-1}B'K).$$

2. Stochastic Case: White Noise Perturbations.

We now wish to consider the case where the plant is disturbed by an independent increments (white noise) input. Before doing this, however, we will generalize the results of the previous section by permitting the initial disturbance x_o to be stochastically selected rather than deterministic. In particular,

$$E\{x_o\} = 0 \; ; \; E\{x_o x_o'\} = W>0 \tag{17}$$

where E is an expectation operator over the probability-measure space of x_o and W is positive semi-definite.

The cost functional to be considered is

$$J = \frac{1}{2}\int_0^\infty E\{u'Ru+x'Qx\}\,dt. \tag{18}$$

The integration and expectation operators may be interchanged so that

$$J_1 = \frac{1}{2}\,E\left\{\int_0^\infty [u'Ru+x'Qx]dt\right\} = J \tag{19}$$

if the integrand of Eq. (18) is integrable, i. e., J exists, and if the argument of the expectation operation in Eq. (19) is finite with probability one.

We will constrain the optimal feedback controller to be a member of the set of linear time-invariant dynamic systems. (Under the

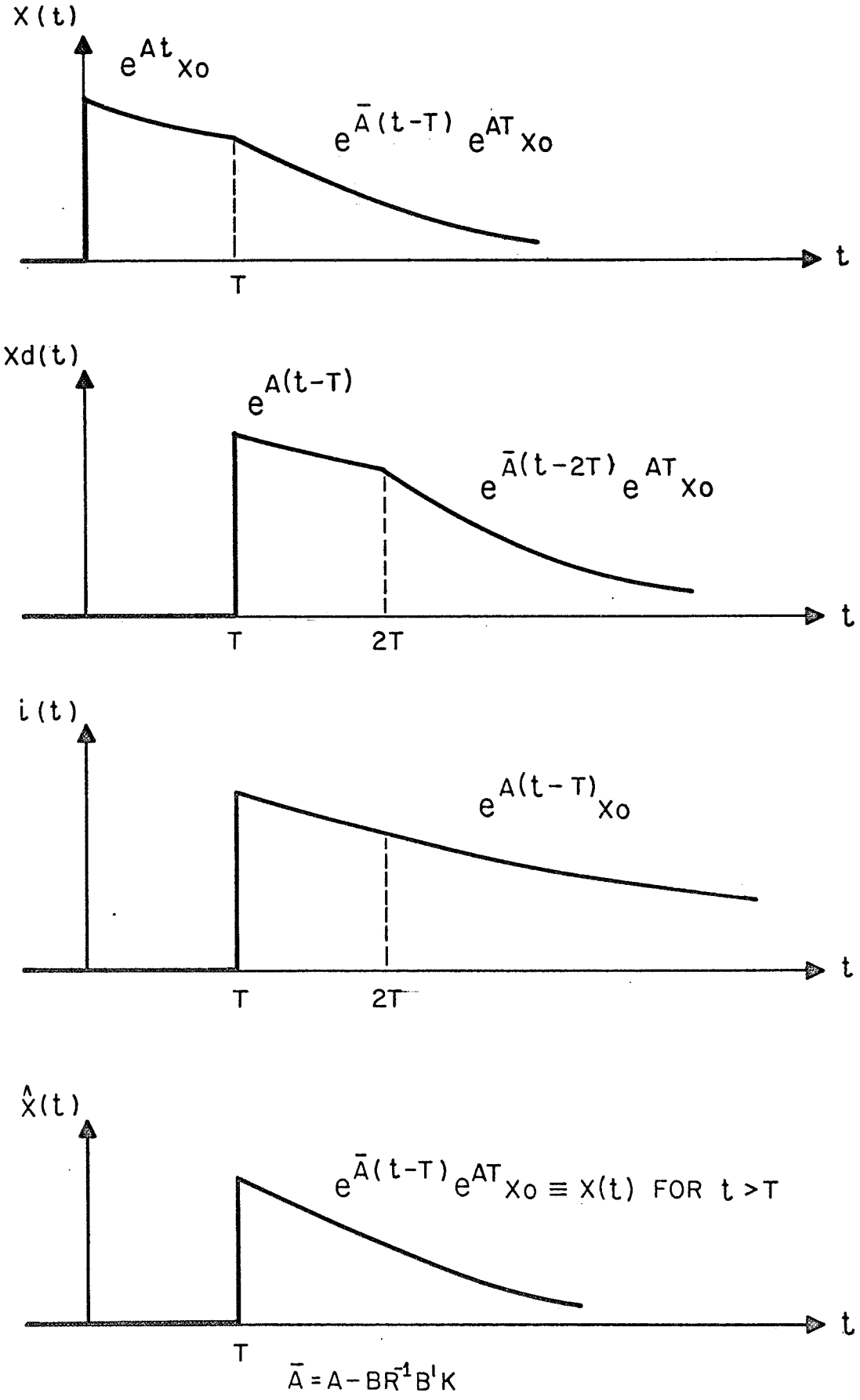

FIG. 4 REPRESENTATIVE BEHAVIOR OF ESTIMATOR

additional assumption that the disturbance input random variables are gaussian, this linear time-variant controller can be shown to be as good as any non-linear or time-varying controller which is also realizable and operates exclusively on $x_d(t)$.)

The control situation is shown in Fig. 5. The disturbance input is $w(t) = x_o\delta(t)$ (a vector-valued impulse), and the feedback controller is constrained to be linear time-invariant, so the Green's function or impulse response for the closed-loop system relating $x_d(t)$ to $w(t)$ may be denoted as $\Phi_1(t)$ and that relating $u(t)$ to $w(t)$ as $\Phi_2(t)$:

$$x_d(t) = \int_{-\infty}^{\infty}\Phi_1(T)w(t-T)\,dT \;;\; u(t) = \int_{-\infty}^{\infty}\Phi_2(T)w(t-T)\,dT \qquad (20)$$

where

$$\Phi_1(T) = \Phi_2(T) = 0 \text{ for } T<T.$$

The cost

$$J = \frac{1}{2}\int_0^{\infty} E\{\iint_0^{\infty} w'(t-T_1)\Phi_2'(T_1)R\Phi_2(T_2)w(t-T_2)dT_1dT_2\} + E\{\iint_0^{\infty} w'(t-T_1)\Phi_1'(T_1)Q\Phi_1(T_2)w(t-T_2)dT_1dT_2\}dt \; . \qquad (21)$$

Assuming that the expectation operator will commute with the inner double integration, noting that the inner integrand is a scalar and may be written as the trace of a 1x1 matrix, and remembering that $tr(ABC) = tr(BCA) = tr(CAB)$, the cost may be rewritten

$$J = \frac{1}{2}\int_0^{\infty}\{tr\iint_{-\infty}^{\infty}\Phi_2'(T_1)R\Phi_2(T_2)E\{w(t-T_2)w'(t-T_1)\}dT_1dT_2 + tr\iint\Phi_1'(T_1)Q\Phi_1(T_2)E\{w(t-T_2)w'(t-T_1)dT_1dT_2\}dt \qquad (22)$$

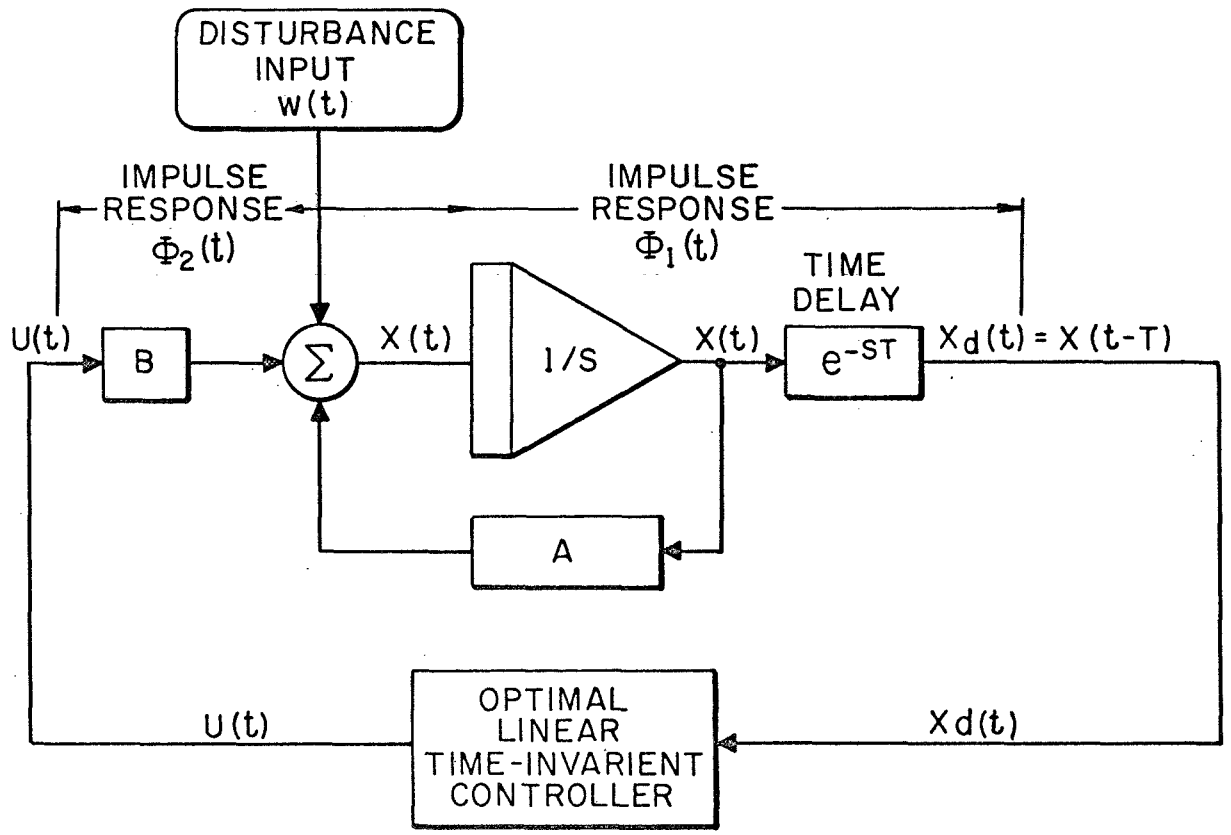

$$X_d(t) = \int_{-\infty}^{\infty} \Phi_1(\tau)\, w(t-T)\, d\tau$$

$$U(t) = \int_{-\infty}^{\infty} \Phi_2(\tau)\, w(t-\tau)\, d\tau$$

$\Phi_1(\tau) = \Phi_2(\tau) = 0$ FOR $\tau < T$.

FIG. 5 SYSTEM DIAGRAM WHEN CONTROLLER IS CONSTRAINED TO BE LINEAR AND TIME INVARIANT

Substituting

$$E\{w(t-T_2)w'(t-T_1)\} = W\delta(t-T_1)\delta(t-T_2),$$

$$J = \frac{1}{2}\int_0^\infty tr[\Phi_2'(t)R\Phi_2(t)\ W + \Phi_1'(t)Q\Phi_1(t)W]dt. \qquad (23)$$

Having eliminated all random variables from the cost expression, we have the same expression to be minimized as we would have in the following problem:

$$x_o \text{ deterministic }, \ x_o x_o' = W$$

$$J = \frac{1}{2}\int_0^\infty [u'Ru + x'Qx]dt. \qquad (24)$$

Note that $\Phi_1(t)$, $\Phi_2(t)$ have been constrained to represent Green's functions indicated in Fig. 5. In particular, $\Phi_1(t) = \Phi_2(t) = 0$ for $t<T$. This problem was solved in the previous section, and resulted in the controller of Fig. 3. We have shown that the same cost functional is to be minimized subject to the same constraints in the stochastic initial disturbance case as in the deterministic initial disturbance case. The controller of Fig. 3 is thus the optimal linear time-invariant controller for either a stochastic or deterministic initial disturbance.

Now we consider a (white noise) disturbance process W(t) composed of independent increments, such that

$$E\{w(t)\} = 0 \ ; \ E\{w(t)\}w'(t+T)\} = W\delta(T). \qquad (25)$$

The cost functional selected is

$$J = \lim_{T\to\infty} \frac{1}{2T} \int_0^T E\{u'Ru+x'Qx\}dt \tag{26}$$

therefore

$$J = \lim_{T\to\infty} \frac{1}{2T} \int_0^T \{tr\int\int_{-\infty}^{\infty} \Phi_2'(T_1)R\Phi_2(T_2)W\ \delta(T_2-T_1)dT_1dT_2 + tr\int\int_{-\infty}^{\infty} \Phi_1'(T_1)Q\Phi_1(T_2)W\delta(T_2-T_1)\ dT_1\ dT_2\}dt \tag{27}$$

The integrand is a constant independent of t, so the operator

$$\lim_{T\to\infty} \frac{1}{T} \int_0^T dt$$

is the identity operator.

Using the fact that $\Phi_2(T_1) = \Phi_1(T_1) = 0$ for $T_1 < 0$,

$$J = \frac{1}{2} \int_0^{\infty} tr[\Phi_2'(t)R\Phi_2(t)W + \Phi_1'(t)Q\Phi_1(t)W]dt. \tag{28}$$

This is exactly the same cost functional seen in the two previous cases (deterministic and stochastic initial disturbances) and $\Phi_1(t)$ and $\Phi_2(t)$ are under the same constraints. The controller of Fig. 3 is the optimal linear time-invariant controller for this stochastic regulator task also.

It can be shown that $\hat{x}(t)$ is the least-squares (minimum variance) estimate of the state of the plant integrators $x(t)$ given $x_d(T)$, $T < t$. This is done by showing that

$$E\{[x(t) - \hat{x}(t)]\hat{x}'(t)\} = 0 \ ,$$

i.e., that the error in the estimate is uncorrelated with the estimate. If we now make the assumption that the input process is strongly stationary gaussian white noise, x(t) and $\hat{x}(t)$ will also be gaussian random variables (Ref. 11) in which case the fact that error and estimate are uncorrelated implies that they are statistically independent. This linear time-invariant estimator which develops $\hat{x}(t)$ is then the best of all possible estimators, i.e. there is no nonlinear or time-varying estimator which provides a lower variance estimate of x(t).

Thus in the case of white noise perturbation, the optimal controller again separates into an estimator, (which is the optimal minimum-variance estimator when the input noise is gaussian) followed by a controller gain matrix identical to that of the optimal controller when the plant does not contain any time delay.

D. SPECIFIC EXAMPLE: SINGLE INTEGRATOR PLANT WITH TIME DELAY

1. Performance of Optimal Controller

The specific control task evaluated experimentally was compensatory control of a single integrator perturbed by a gaussian white noise input. The equations were:

$$\dot{x} = u \ ; \ J = \lim_{T\to\infty} \frac{1}{2T} \int_0^T E\{\rho u^2 + x^2\}dt \qquad (29)$$

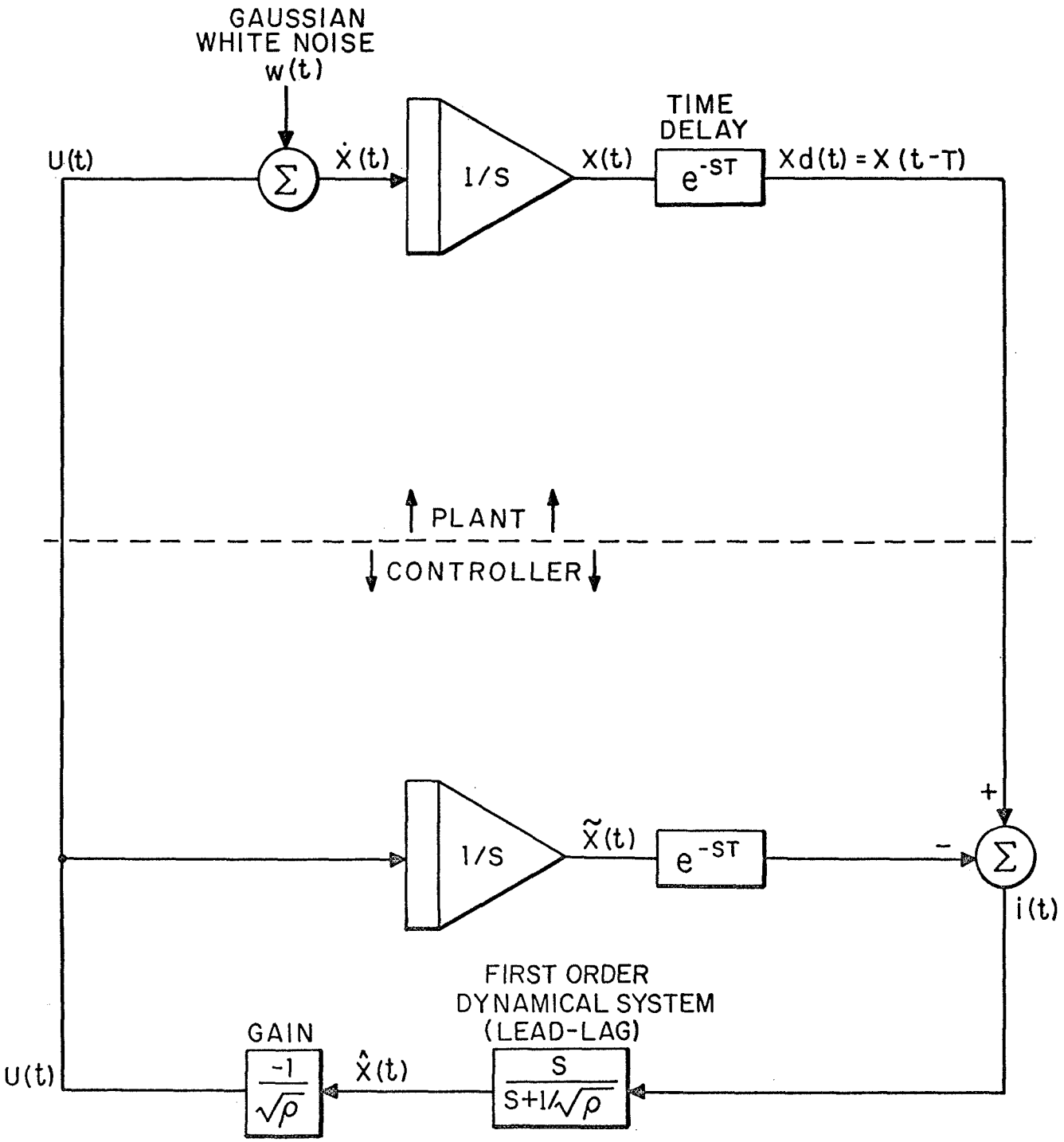

FIG. 6 OPTIMAL CONTROLLER FOR SINGLE INTEGRATOR WITH TIME DELAY

The Riccati equation is thus a scalar relation:

$$0 = 1 - \frac{K^2}{\rho} \quad \text{or} \quad K = \sqrt{\rho}. \tag{30}$$

The optimal control is thus $u(t)^* = -\hat{x}(t)/\sqrt{\rho}$, and the corresponding structure is shown in Fig. 6.

The steady-state performance may be calculated for $E\{w(t)w'(t+T)\} = \delta(T)$:

$$\begin{aligned}\lim_{T\to\infty} \frac{1}{2T} \int_0^T E\{u^2\}dt &= \frac{1}{2} \int\int_{-\infty}^{\infty} \Phi_2(T_1)\Phi_2(T_2)\delta(T_1-T_2)dT_1dT_2 \\ &= \frac{1}{2} \int_0^{\infty} \Phi_2^2(t)dt\end{aligned} \tag{31}$$

and

$$\begin{aligned}\lim_{T\to\infty} \frac{1}{2T} \int_0^T E\{x^2\}dt &= \frac{1}{2}\int\int \Phi_1(T_1)\Phi_1(T_2)\delta(T_1-T_2)dT_1dT_2 \\ &= \frac{1}{2} \int_0^{\infty} \Phi_1^2(t)dt\end{aligned} \tag{32}$$

where $\Phi_1(t)$ and $\Phi_2(t)$ are the functions shown in Fig. 7. Therefore,

$$\lim_{T\to\infty} \frac{1}{2T} \int_0^T E\{x^2\}dt = \frac{T}{2} + \frac{\sqrt{\rho}}{4}$$

and (33)

$$\lim_{T\to\infty} \frac{1}{2T} \int_0^T E\{u^2\}dt = \frac{1}{4\sqrt{\rho}}$$

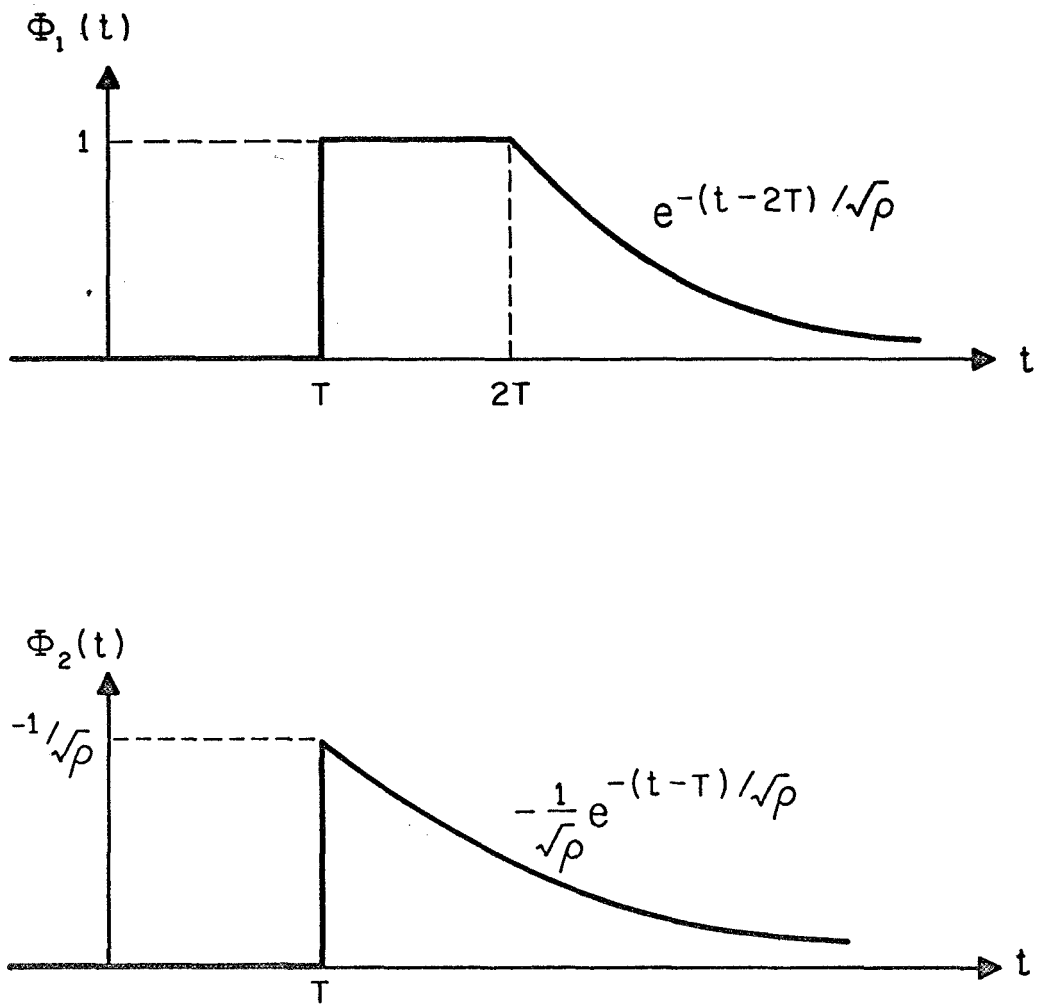

FIG. 7 IMPULSE RESPONSES $\Phi_1(t)$ AND $\Phi_2(t)$ FOR SINGLE-INTEGRATOR SYSTEM

Eliminating ρ, we have the optimal trade-off between $\overline{x^2}$ and $\overline{u^2}$

$$\frac{\overline{x^2}}{2} = \frac{T}{2} + \frac{1}{16}\left(\frac{\overline{u^2}}{2}\right)^{-1} \tag{34}$$

The performance curve, $\frac{\overline{x^2}}{2}$ versus $\frac{\overline{u^2}}{2}$, is plotted with ρ as a parameter in Fig. 8.

2. Comparison With a Simple Suboptimal Controller

The transfer function of the entire controller of Fig. 6 is

$$H(s) = \frac{-s}{1+\sqrt{\rho}\ s\ -e^{-sT}} \ . \tag{35}$$

Plots of the magnitude and phase of H(s) for T = .2, a typical value for the human controller, are shown in Fig. 9. Note that when ρ is near unity, a reasonable value H(s) behaves approximately like a simple gain at low frequencies and another simple gain at high frequencies. The asymptotes of the gain are:

$$\begin{aligned} \lim_{s\to 0} H(s) &= \lim_{s\to 0} \frac{-s}{1+\sqrt{\rho}\ s\ -\ e^{-sT}} = \frac{-1}{T+\sqrt{\rho}} \\ \lim_{s\to \infty} H(s) &= \lim_{s\to \infty} \frac{-s}{1+\sqrt{\rho}\ s\ -\ e^{-sT}} = \frac{-1}{\sqrt{\rho}} \end{aligned} \tag{36}$$

H(s) can thus be approximated quite closely both in magnitude and phase as a lead-lag network with low frequency gain $-1/(T + \sqrt{\rho})$, high frequency gain $-1\sqrt{\rho}$, and high frequency pole at $s \approx -2\pi/T = 15.7$ for a ρ of unity or larger.

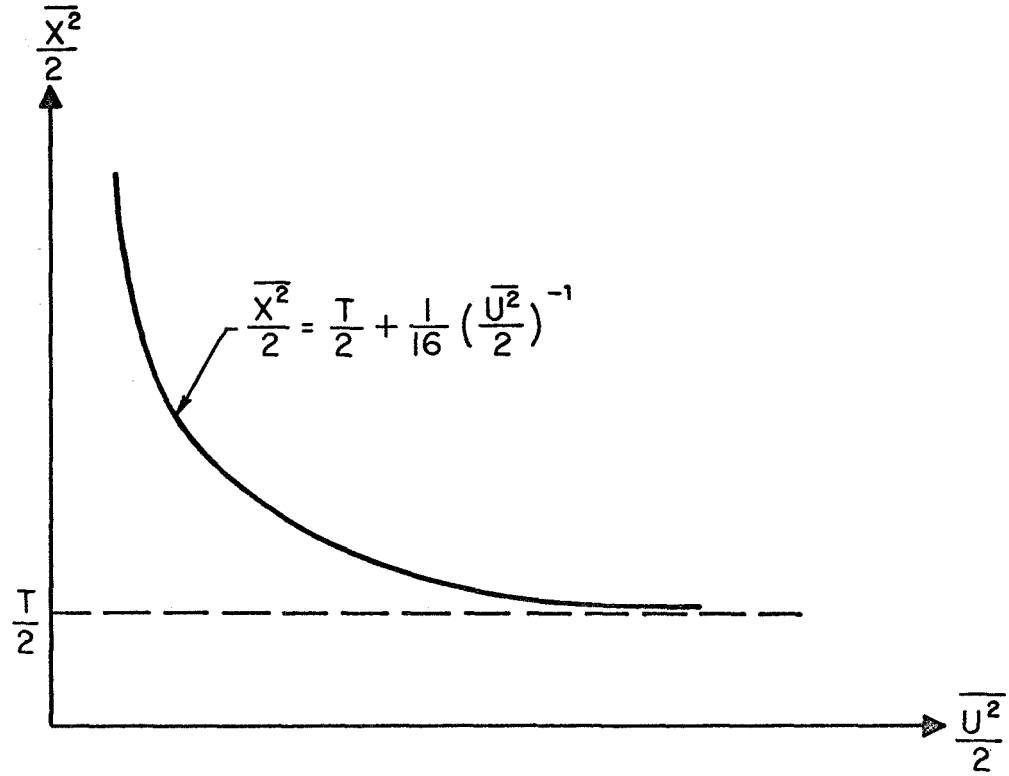

$$\frac{\overline{X^2}}{2} = \frac{T}{2} + \frac{\sqrt{\rho}}{4} \; ; \; \frac{\overline{U^2}}{2} = \frac{1}{4\sqrt{\rho}}$$

FIG. 8 PERFORMANCE OF OPTIMAL CONTROLLER

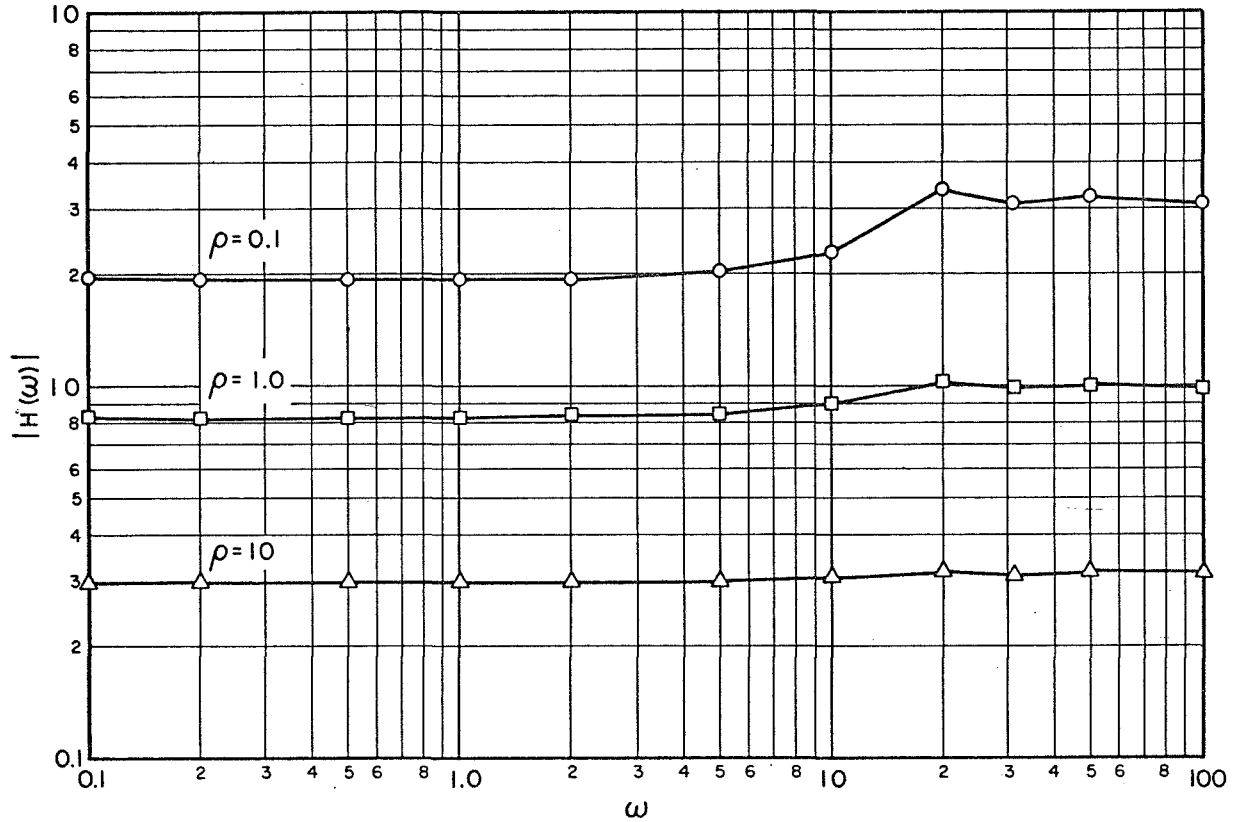

FIG. 9a MAGNITUDE OF OPTIMAL FEEDBACK CONTROLLER

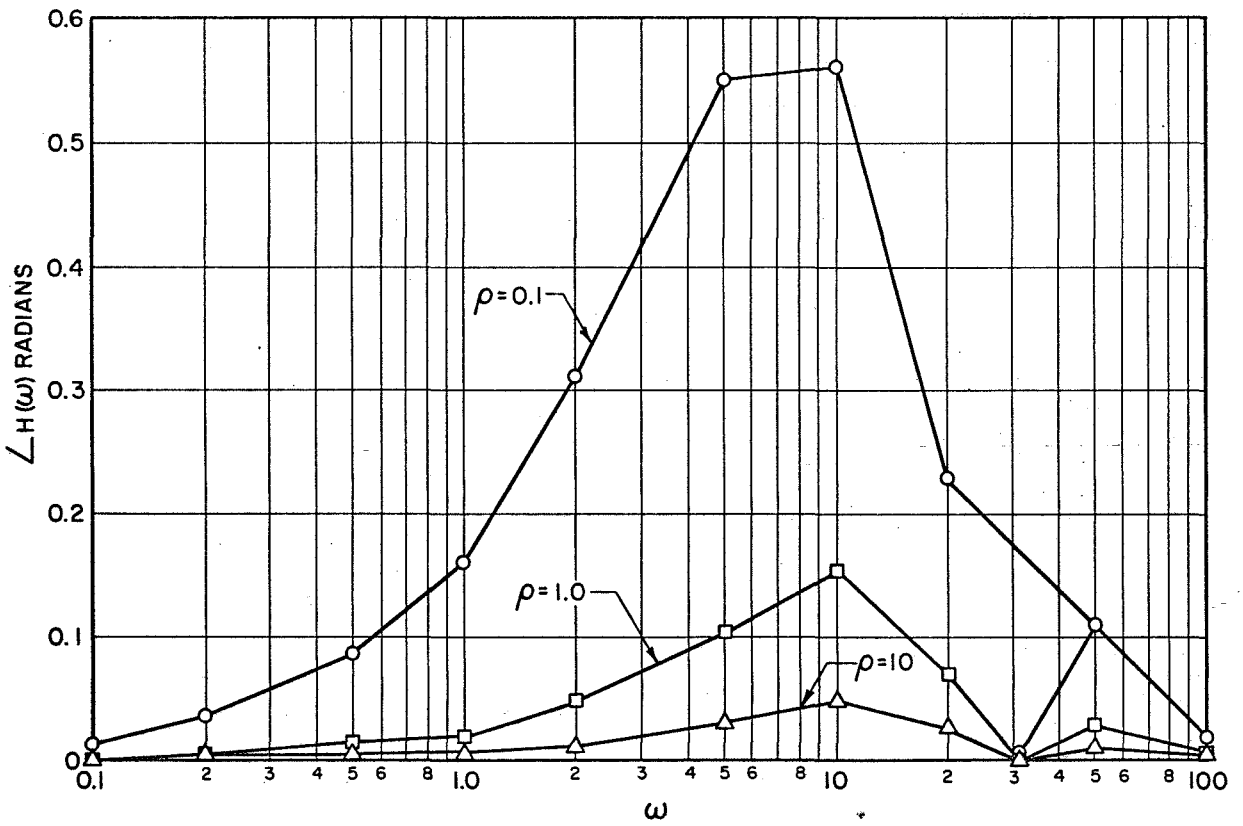

FIG. 9b PHASE OF OPTIMAL FEEDBACK CONTROLLER

This suggests an experiment with a very simple suboptimal control: suppose that instead of the optimal feedback controller, we use a simple gain. How much worse a feedback control strategy is this, that is, how is the $\overline{x^2}/2$ versus $\overline{u^2}/2$ tradeoff curve modified?

To compute the new performance, let the controller gain be denoted as α, and note that the input-to-error impulse response $\Phi_1(t)$ now has transform

$$\Phi_1(s) = \frac{e^{-st}}{s + \alpha e^{-st}} \quad . \tag{37}$$

As before,

$$\frac{\overline{x^2}}{2} = \frac{1}{2}\int_0^\infty \Phi_1^2(t)dt \quad . \tag{38}$$

By Parseval's Theorem

$$\frac{\overline{x^2}}{2} = \frac{1}{2\pi i}\int_{-i\infty}^{i\infty} \Phi_1(s)\Phi_1(-s)ds = \frac{1}{\pi}\int_0^\infty \frac{d\omega}{\omega^2 + \alpha^2 - 2\alpha\omega \sin \omega T} \quad . \tag{39}$$

This is not simply integrable, so we will expand the integrand in a power series in (αT) around the point $(\alpha T) = 0$ and then integrate term by term:

$$\frac{\overline{x^2}}{2} = \frac{1}{4\alpha}\{1+\alpha T + \frac{3(\alpha T)^2}{2} + O[(\alpha T)^2]\} \tag{40}$$

Since $u = \alpha x$, $\overline{u^2}/2 = \alpha^2 \overline{x^2}/2$.

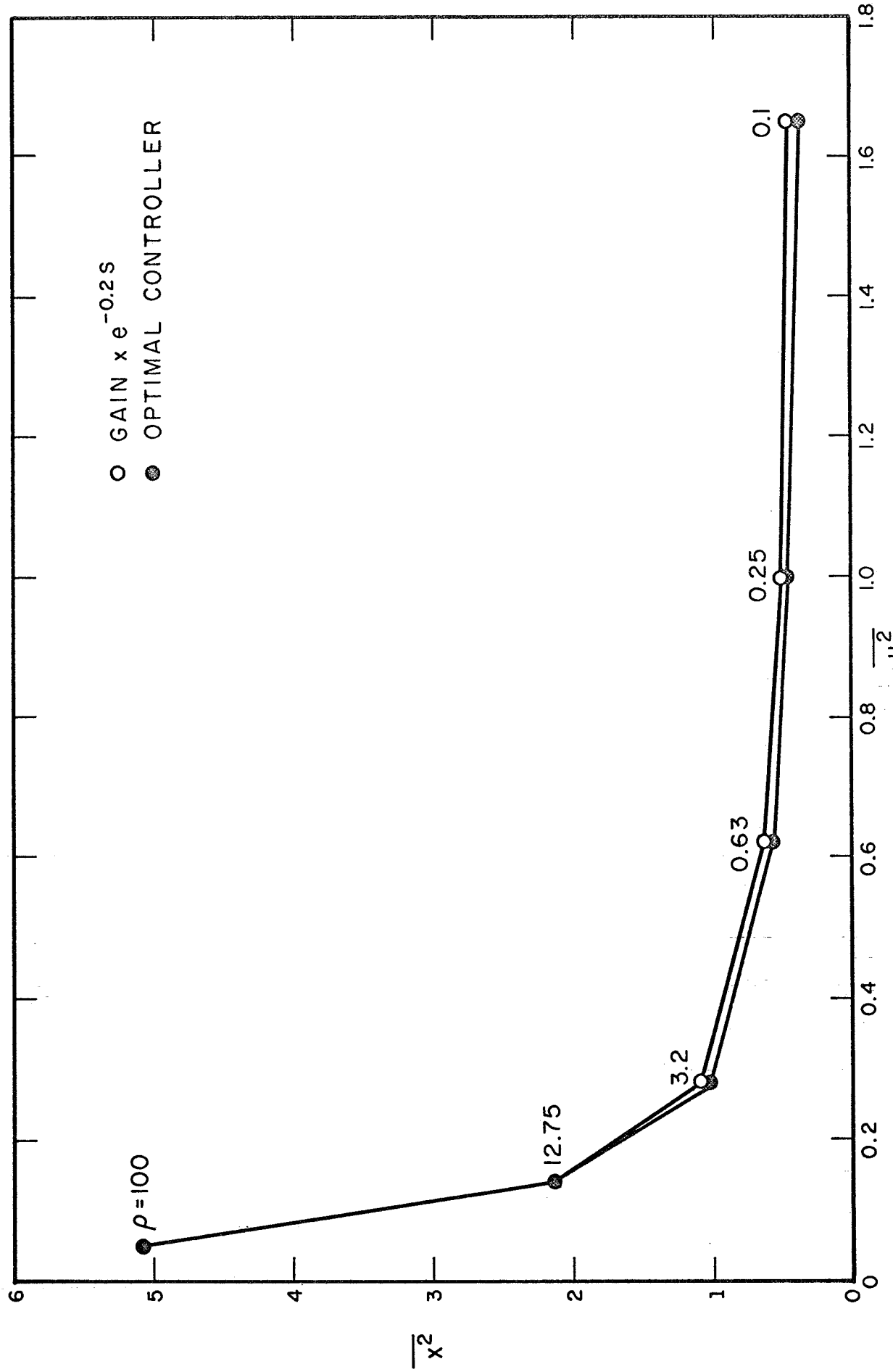

FIG. 10 PERFORMANCE COMPARISON BETWEEN OPTIMAL CONTROLLER AND SIMPLE GAIN WITH DELAY (UNIT POWER DENSITY INPUT)

The suboptimal control performance is plotted in comparison with the optimal in Fig. 10 for T = .2. We see from Fig. 10 that this simple suboptimal strategy performance converges exactly to that of the optimal strategy for large ρ: even for $.1 < \rho < 1$ the two curves are fairly close. However, for $\rho << .1$ the curves diverge. In addition, the simple model is a bad approximation to the optimal for $\rho << .1$, but is reasonably good for larger ρ.

For part of the analysis of the experimental data, we modelled the human controller as a simple gain plus a time delay and found the best value for his equivalent gain. Given measurements of the equivalent gain of the human controller for several values of ρ, we can determine how he adjusts this equivalent gain as a function of ρ. The controller's gain adjustment can then be compared with the optimal adjustment to determine how closely he selects the optimal operating point and how closely he achieves an optimal tradeoff between $\overline{x^2}/2$ and $\overline{u^2}/2$ as ρ changes.

Since

$$J = \overline{x^2}/2 + \rho\, \overline{u^2}/2, \tag{41}$$

the minimization requirement gives

$$dJ = d(\overline{x^2}) + \rho\, d(\overline{u^2}) = 0 \tag{42}$$

The slope of tradeoff curve at the operating point is

$$d(\overline{x^2})/d\overline{u^2} = -\rho \tag{43}$$

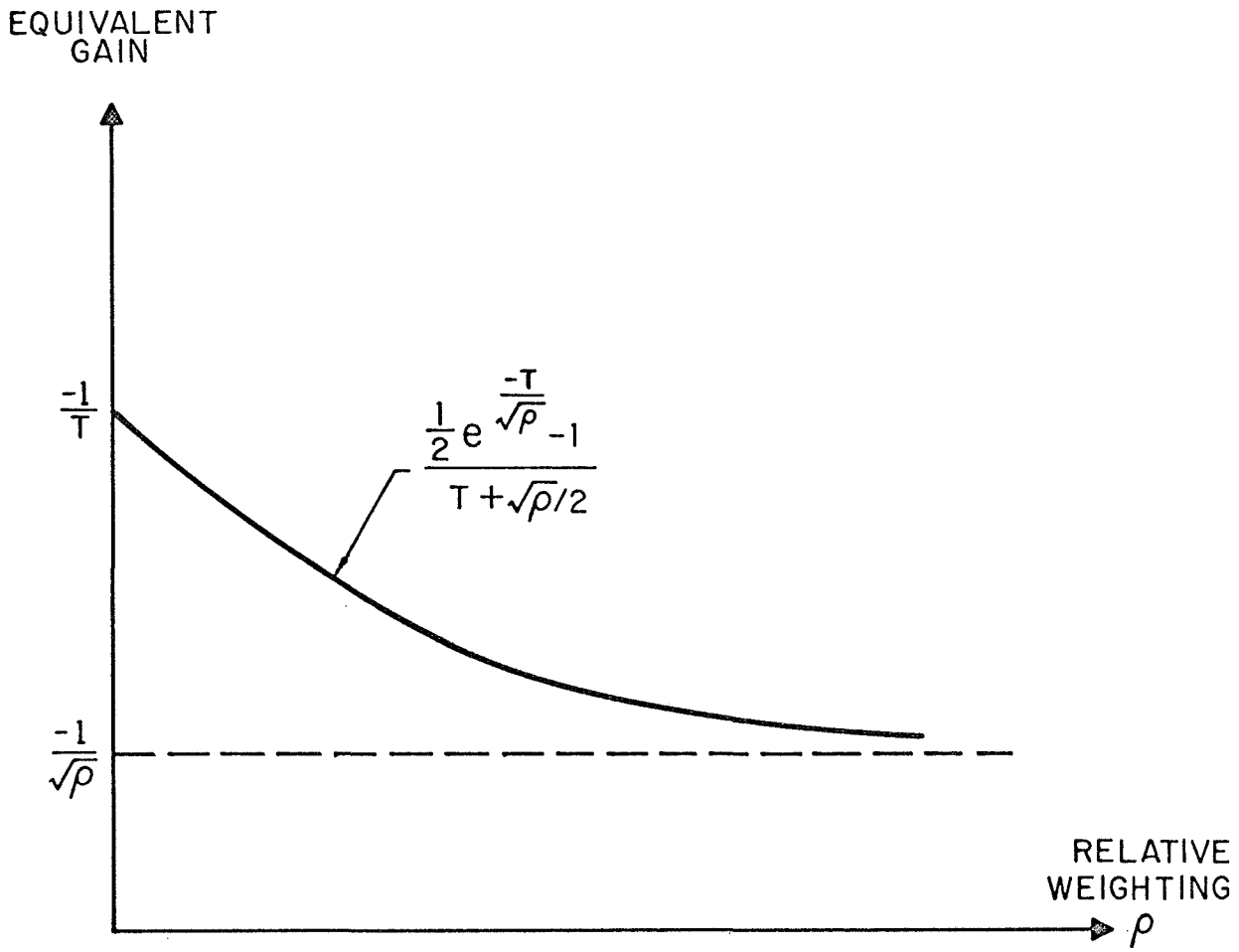

FIG. 11 EQUIVALENT (CROSS-CORRELATION) OPTIMAL GAIN FOR CONTROLLING THE SINGLE INTEGRATOR PLANT

Also, $d^2J>0$, so the tradeoff curve must be concave upward at the operating point, i.e., $d^2(\overline{x^2})/d(\overline{u^2})^2 > 0$.

To compute the equivalent gain of the human, we will take the instantaneous cross-correlation between his input (x_d) and his output (u). In terms of Fig. 6,

$$\alpha = E\{ux_d\}/E\{x^2_d\} \tag{44}$$

where α is the equivalent or cross correlation gain of the human controller. If the optimal controller were in the feedback loop, Eq. (44) would give the following value for the gain:

$$\alpha = \frac{(e^{-T/\sqrt{\rho}} - 1) - \frac{1}{2} e^{-T/\sqrt{\rho}}}{T + \sqrt{\rho}/2} = \frac{\frac{1}{2} e^{-T\sqrt{\rho}} - 1}{T + \sqrt{\rho}/2} \tag{45}$$

This equivalent optimal gain is plotted in Fig. 11 as a function of ρ.

CHAPTER III

DESCRIPTIONS OF EXPERIMENT

A. INTRODUCTION

In the previous chapter we developed an optimal control model for the human controller. We used this model to determine the optimal equivalent gain as a function of ρ, the relative weighting of control $\overline{u^2}/2$ and error $\overline{x^2}/2$ and to determine the optimal trade-off between $\overline{u^2}/2$ and $\overline{x^2}/2$ as a function of ρ. In this chapter we describe the experiments that we performed to test this model. In these experiments we attempted to determine how close to optimal the human control set his equivalent gain and how close to optimal was his trade-off between $\overline{u^2}/2$ and $\overline{x^2}/2$ as the relative weighting ρ was changed. The experiments were of limited scope and in a sense should be considered to be pilot experiments. Only one subject was used, but he was very carefully trained in all conditions.

The experimental control system was a modified compensatory system with gaussian input disturbance. The block diagram of the system is in Fig. 12. The principal difference between our control situation and the conventional compensatory situation was that the subject was instructed to minimize a cost functional or score that was the weighted sum of the mean-squared error and of the mean-squared control movements.

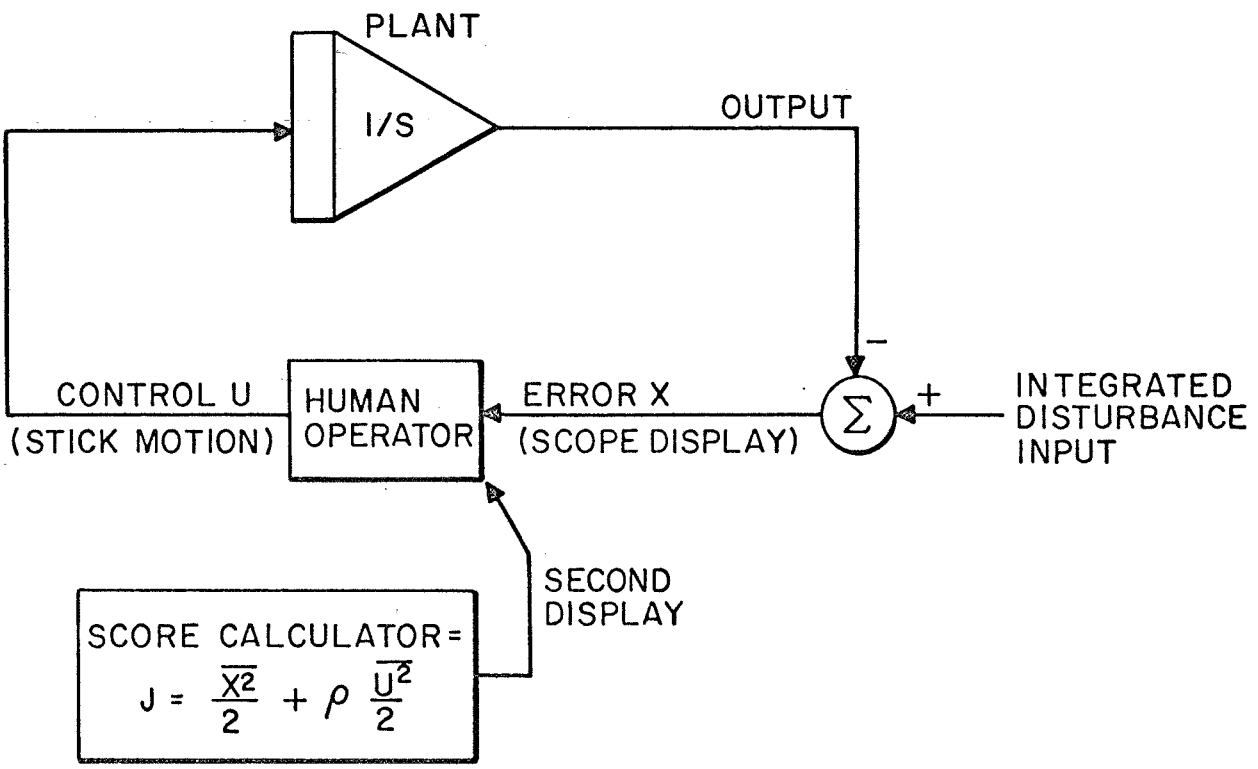

FIG. 12 BLOCK DIAGRAM OF EXPERIMENTAL SYSTEM

This meant that, in general, he should have used somewhat smaller control movements and incurred a greater mean-squared error than he would have if he were scored on mean-squared error alone. To help the controller optimize his behavior, he was given explicit feedback of his running score by a "cost circle" display. This was similar to the technique used by Miller (Ref. 10) in a previous study of the optimality of human controller behavior.

B. APPARATUS

The subject was seated in a small, acoustically insulated room, facing an oscilloscope screen and a control stick. The room light intensity was adjusted to his comfort and then held constant. He was seated in a dentist's chair with a headrest adjusted so that his eyes were on a level with the screen and were approximately 72 cm. away.

The diameter of the oscilloscope screen was 12 cm. The screen contained three time-shared signals, so that the display appeared as shown in Fig. 13. The electronic switches which time-shared the display signals ran at 60 and 30 Hz, so that the entire display was repeated 30 times per second. Thus the time per display frame was 33.3 milliseconds. The frame time was allocated in the following manner: 16.7 milliseconds was spent displaying the error dot, whose vertical displacement from the center of the screen represented tracking error; 8.3 milliseconds was spent displaying a target circle which was 0.5 cm. in diameter and was located at the center of the screen; and 8.3 milliseconds was spent displaying a scoring circle. The diameter of the scoring circle was proportional to the subject's instantaneous score processed by a first-order lag filter with a time constant of 2 seconds.

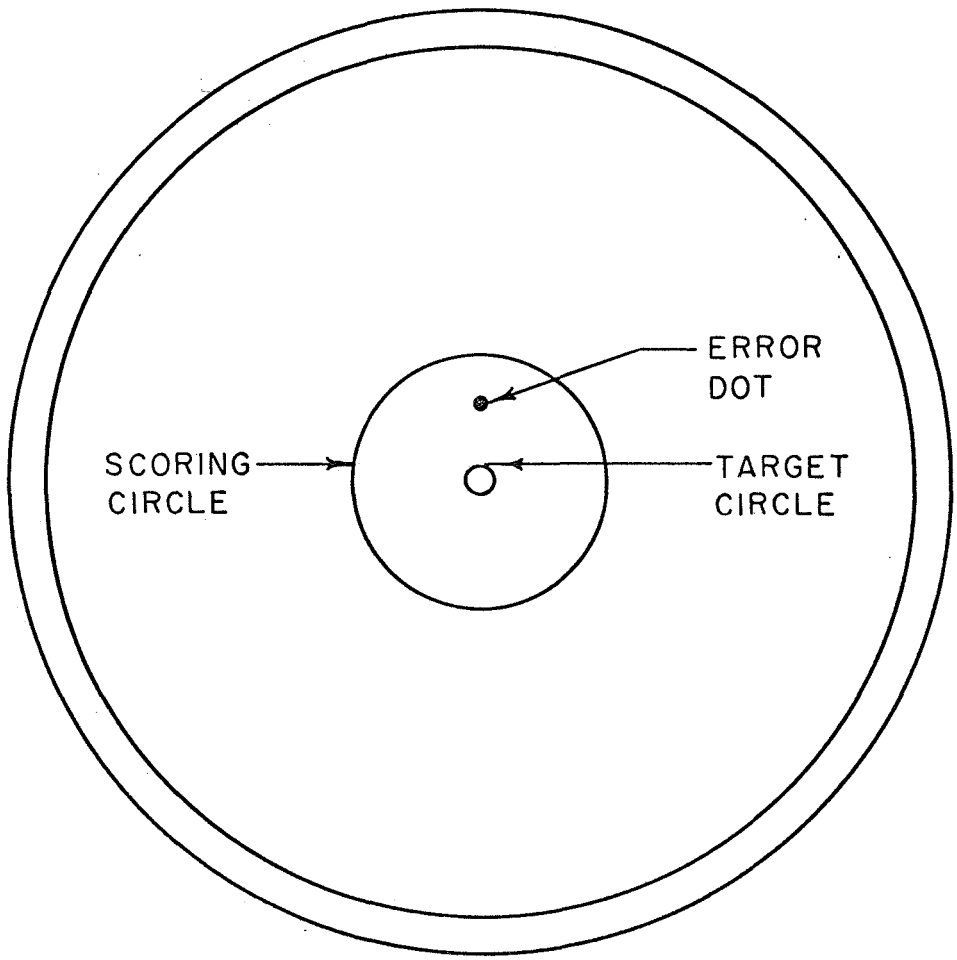

FIG. 13 DISPLAY (TARGET CIRCLE FIXED, ERROR DOT MOVES VERTICALLY, DIAMETER OF SCORING CIRCLE = 2 SEC. AVERAGE OF COST (SCORE) RATE.)

The subject grasped the control device which was an 11-inch long aluminum stick attached to a Measurement Systems Inc. Model 435 force-sensitive hand control. He manipulated the control with the fingers of his right hand. The control was oriented so that the stick was horizontal and could be moved left-right and up-down in a plane parallel to the oscilloscope screen. Only the up-down movements controlled the error dot.

The controlled dynamics was a single integrator, calibrated so that an upward force of 10^5 dynes (1 Newton) on the stick resulted in an upward velocity of the error dot of 6.4 cm/sec on the screen. This upward force displaced the end of the stick approximately 0.1 cm.

The input signal was recorded on magnetic tape and consisted of integrated Gaussian white noise. The input amplitude was adjusted so that its mean-square was 10 cm^2. The procedures by which this tape was generated are discussed in Appendix A. On a second channel of the tape, a control signal was recorded, by means of which the scoring integrators could be started, stopped, and reset at the desired times. The input entered the system at the input to the plant as shown in Fig. 12. Because it was integrated white noise, this input was equivalent to a white noise disturbance of the plant output shown in Fig. 6.

An Electronic Associates Inc. TR-48 analog computer with associated peripheral equipment was used to generate the display seen by the subject, to provide the controlled dynamics, and to compute scores for each run. The score for a run was the weighted sum of the mean-squared error and the mean-squared stick movement normalized by dividing by the mean-squared input. The relative weighting for

the score was, of course, the same as the weighting used for the scoring circle. The input, error, and stick movement signals which occurred during a run were monitored and recorded on magnetic tape by means of a Technical Measurement Corp. Mnemotron FM tape recorder.

C. EXPERIMENTAL PROCEDURE

The subject used was highly-experienced at various manual control tasks. He was instructed that he was to carry out a velocity control compensatory tracking task in such a manner as to minimize his total score as indicated by the diameter of the scoring circle on the screen. He was told that his score would consist of a weighted sum of his mean-squared stick movement and the mean-squared error.

Runs were taken in blocks of four. Because of the control signal recorded on the input tape, the same four input segments were repeated for each block. This insured that each block was of exactly the same difficulty, so that scores could be compared from block to block in order to discover how well the subject was learning the task. In order to discourage the subject from memorizing the input signals, the four input segments were presented in random order during each block.

Each of the four runs in a block consisted of 30 seconds of unscored practice and 90 seconds of scoring. At the beginning of each scored segment, the recorded control signal started the scoring integrators. At the end of the scored segment, it turned them off. The experimenter read each score and then reset the

integrators by means of a switch. The subject was allowed to rest approximately one minute between runs in a block and approximately 10 minutes between blocks.

The subject was trained in the tracking task with three cost functions whose stick weighting coefficients, ρ, were 0, 0.1, and 1, respectively. For each of these cases, the subject was trained until his score stabilized, at which time a data block was run. The input, error, and stick movement signals were recorded along with the control level signal which indicated the portion of the run which was being scored.

CHAPTER IV

EXPERIMENTAL RESULTS

A. PERFORMANCE SCORES

In Fig. 14 are plots of the scores $\overline{x^2}$ versus $\overline{u^2}$ with ρ as a parameter for the optimal controller of Fig. 6, and for the human controller. The time delay for the optimal controller was chosen to be 0.2 sec. The human controller results were obtained from the experiments for values of $\rho = 0$, .1 and 1.

The measured points for the human controller lie very close to the $\overline{x^2}$ versus $\overline{u^2}$ trade-off curve for the optimal controller. However, it is apparent from the figure that the human controller did not select the proper operating point to minimize his total score. In particular, he did not move as large a distance along the trade-off curve as did the optimal controller.

B. GAIN ADJUSTMENT

If we assume the suboptimal model consisting of a gain in cascade with a time delay of 0.2 seconds, rather than the more complex optimal controller model of Fig. 6, we can determine the best fit gain from records of the error and control movements. To find the best fit linear gain for this model, a regression analysis

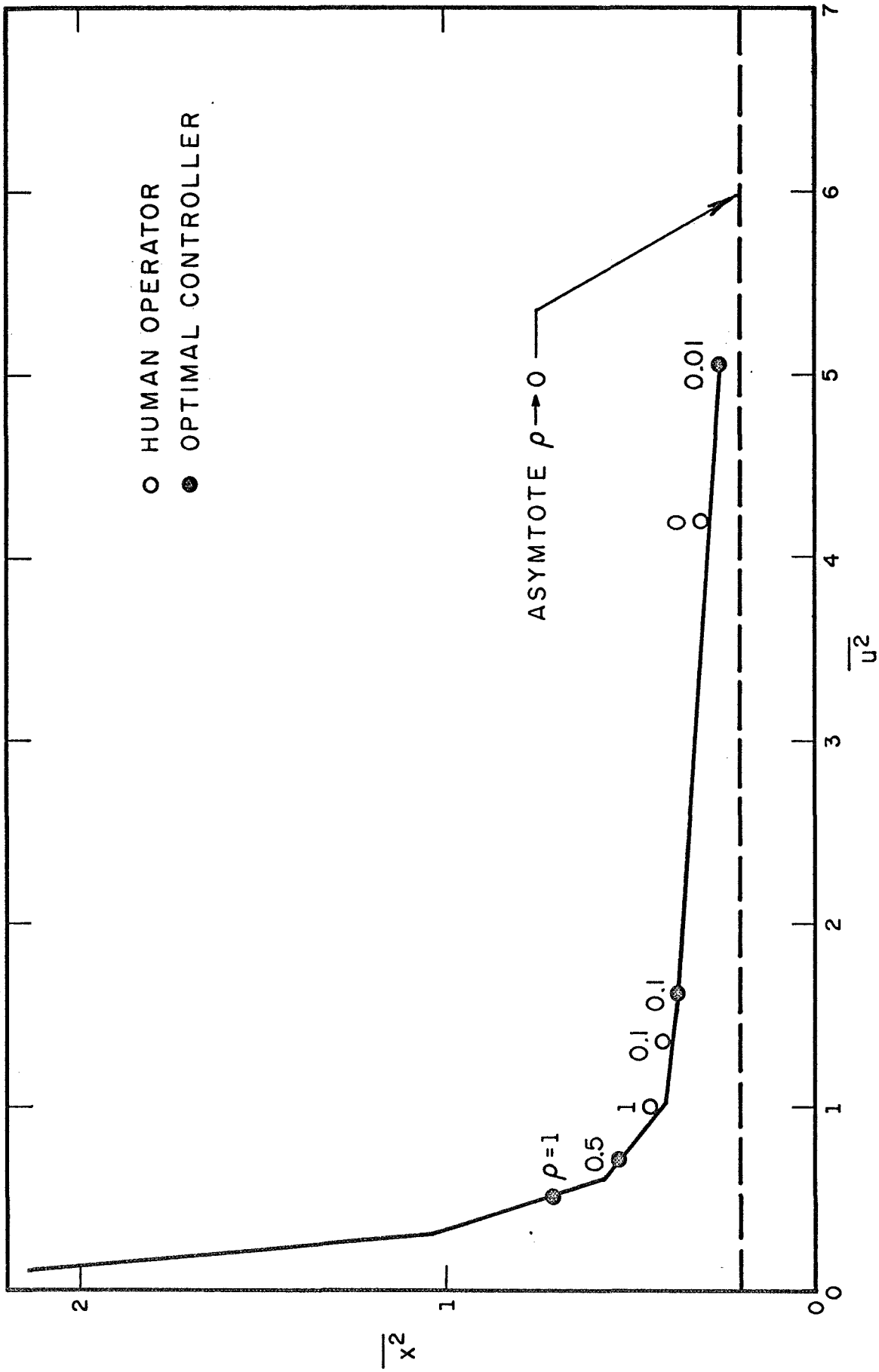

FIG. 14 COMPARISON BETWEEN HUMAN OPERATOR AND OPTIMAL CONTROLLER WITH TIME DELAY 0.2 SECONDS.

was performed. This analysis consisted of measuring the mean value of $u^2(t)$, $x^2(t-T)$, and $u(t)x(t-T)$ over the four runs recorded when $\rho = .1$, and again over the four for $\rho = 1$.

Assuming all variables are gaussian, the minimum variance estimate of the human operator's equivalent gain is

$$G = \frac{\overline{u(t)x(t-T)}}{\overline{x^2(t-T)}} \tag{46}$$

The correlation coefficient between u(t) and x(t-T) is

$$r = \frac{\overline{u(t)x(t-T)}}{\sqrt{\overline{u^2(t)}\ \overline{x^2(t-T)}}} \tag{47}$$

If the same experiment were performed with the optimal controller replacing the human, we would expect to measure an equivalent

$$G_o = \frac{\overline{u(t)x(t-T)}}{\overline{x^2(t-T)}} = \frac{1 - \frac{1}{2}e^{-T/\sqrt{\rho}}}{T + \sqrt{\rho}/2} \tag{48}$$

and a correlation coefficient of

$$r_o = \frac{1 - \frac{1}{2}e^{-T/\sqrt{\rho}}}{\frac{1}{2}\sqrt{1 + 2T/\sqrt{\rho}}}$$

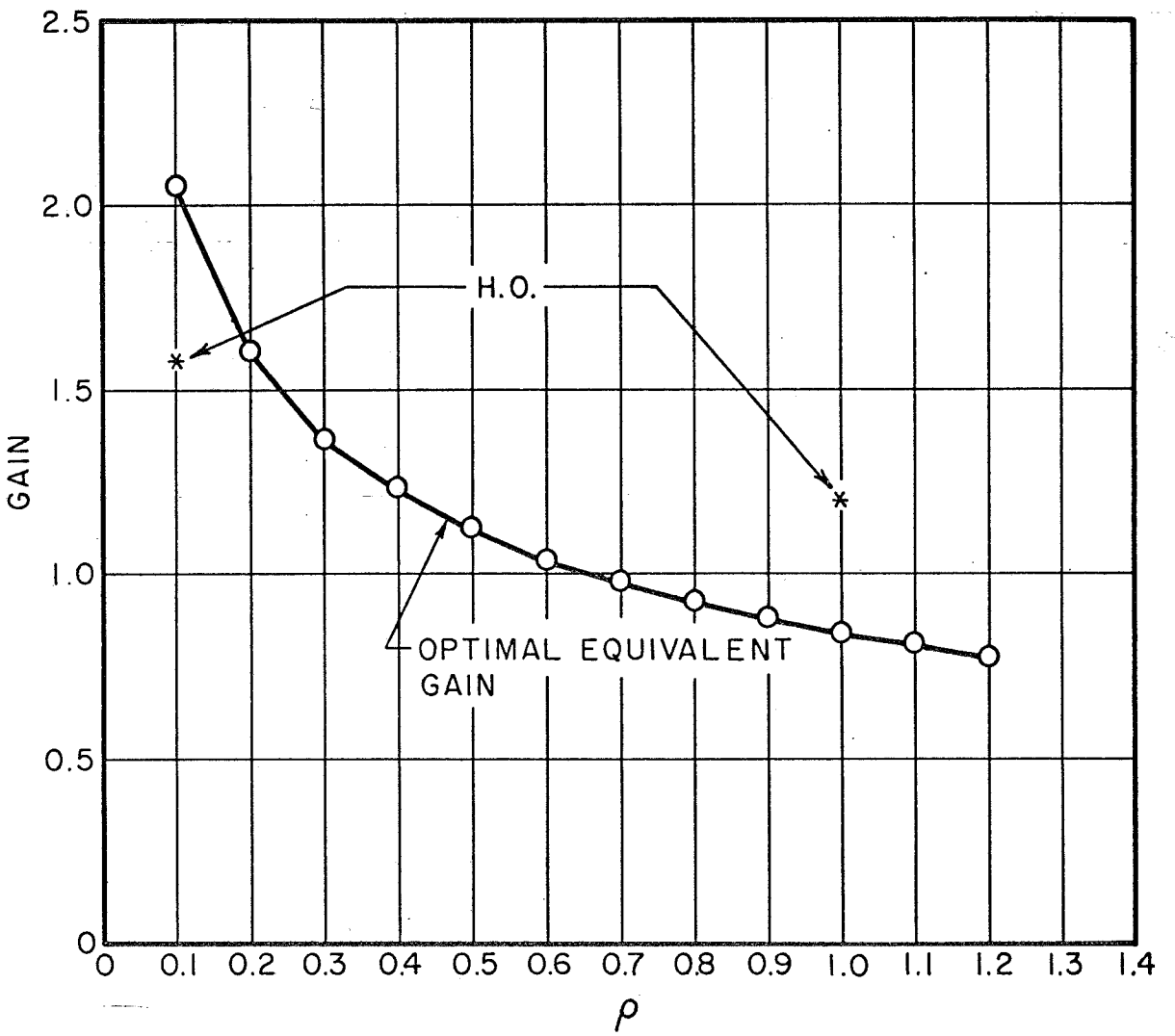

FIG. 15 COMPARISON BETWEEN EQUIVALENT GAIN OF HUMAN OPERATOR AND EQUIVALENT GAIN OF OPTIMAL CONTROLLER.

A comparison between this optimal equivalent gain and the measured gain is in Fig. 15. We see that the human had a gain lower than optimal for $\rho = .1$ and higher than optimal for $\rho = 1$. The correlation coefficients obtained were $r = .88$ for $\rho = .1$ and $r = .85$ for $\rho = 1$. These were somewhat lower than the .98 and .99 that would have been measured with the optimal controller in the circuit.

C. DISCUSSION

There are two reasons for the difference between the behavior of the optimal controller and of the human controller. First, in deriving the optimal controller we may have made incorrect assumptions about the human controller's characteristics. Second, the human controller's subjective estimates of ρ may have differed from the actual values used in the experiment.

Our assumption that the human controller's time delay T was 0.2 second is one possible source of disagreement between the human controller and the optimal model. The effect of T on the tradeoff curve is given by Eq. (34) which states that

$$\frac{\overline{x^2}}{2} = \frac{T}{2} + \frac{1}{16}\left(\frac{\overline{u^2}}{2}\right)^{-1} \qquad (50)$$

T thus has the effect of translating the tradeoff curve. Since the experimental points lie almost on the tradeoff curve for the optimal controller shown in Fig. 14, for which T = 0.2 second, we may conclude that this value of T is approximately correct. Moreover, changing T would not result in a better agreement between

the human controller's operating points and those of the optimal controller. In particular, a change of T would not account for the fact that the operating point for the optimal controller moves much further along the trade-off curve as ρ changes than did the operating point for the human controller.

A second assumption that might account for the disagreement is the neglection of the human controller's remnant in developing the optimal model. But in these experiments the remnant constituted only a small fraction of the human controller's output. For ρ = 1 and .1, the coefficients of linear correlation between the human controller's output u(t) and his input x(t) were approximately .85 and .88, respectively. Remnant can be modelled by adding a small amount of independent noise to the output of the optimal model to obtain the response u. This noise represents the part of the human operator's response that is uncorrelated with his input. However, the level of the additive noise is low and its effect on the u^2 versus x^2 trade-off curve (Fig. 14) would be small.

Thus, it seems more reasonable to attribute that difference between human and optimal controller behavior to the human controller's misestimation of ρ, the relative weighting of control and error. We should not be surprised to find that the human controller's subjective values of ρ differ from the actual values. The total score is not very sensitive to slight variations in the location of the operating point as long as the operating point remains on the optimal trade-off curve.

In fact, the derivative of cost with respect to the operating point location goes to zero at the optimal location. Since the total cost was rather insensitive to operating point location, the subject would not be highly motivated to find the exact optimal point, and would have a difficult time learning to locate it exactly. His performance might have been improved by additional training, particularly if the additional training was given over a much wider range of ρ values.

Whatever the reason for this lack of adjustment to ρ, it appears that the human operator's performance can be predicted quite well by a model consisting of the optimal structure with parameters chosen to optimize a subjective cost functional that differs from the true one. We can estimate the values of ρ that the human controller optimized for from Figs. 14 and 15. From the trade-off curve of Fig. 14 we can determine the values of ρ that give operating points on the optimal controller's trade-off curve that lie close to the human controller's operating points. Doing this, we find that the human controller apparently optimized for $\rho \sim .02$ rather than the actual value $\rho = 0$, for $\rho \sim .2$ rather than $\rho = .1$ and for $\rho \sim .4$ rather than $\rho = 1$. From the gain versus ρ curve of Fig. 15 we can simply read off the value of ρ for which the equivalent gain of the optimal controller would be the same as the measured gain of the human controller. The values of ρ obtained by this process are $\rho = .2$ and .45 respectively, rather than the actual values $\rho = .1$ and 1. Thus the two sets of empirical values of ρ are in good agreement.

Thus, our results are most simply explained by assuming a subjective weighting ρ_s in the cost functional. For completeness we should also include the remnant in the model for the human controller. The revised model for the human controller would consist of the optimal controller of Fig. 6, with a subjective value of the parameter ρ plus a low-level noise source summed at its output to account for the remnant.

CHAPTER V

CONCLUSIONS

In Chapter II we derived the optimal controller for a plant with quadratic cost functional which takes into account the time delay limitation of the human operator. This optimal controller contains a model of the plant being controlled, plus linear dynamics operating on the difference between the real plant output and the model output.

Such a structure is an excellent model for the human operator. In our experiment with a first-order plant, the human controller's trade-off curve between mean-square error and mean-square control was virtually indistinguishable from the trade-off curve of this optimal controller. However, the human controller did not operate at the point of the trade-off curve which would have minimized his total score. The difference between the operating point and the optimal controller's operating point can be attributed almost entirely to the difference between the human controller's subjective estimate of ρ, the relative weighting of control and error in the cost functional, and the actual weighting. This suggests that the human controller be modelled by the optimal structure with subjective, rather than actual weightings in the cost functional. Understanding how the human controller's subjective weightings are established would appear to be an important problem that deserves considerable attention.

REFERENCES

1. James, H. M., N. B. Nichols and R. S. Phillips. "Manual Tracking" in Theory of Servomechanisms, McGraw-Hill, New York, N. Y., 1947, pp. 360-368.

2. Elkind, J. I. "Characteristics of Simple Manual Control Systems", M.I.T., Lincoln Laboratory, TR 111, 6 April 1956.

3. Wiener, Norbert. Extrapolation, Interpolation, and Smoothing of Stationary Time Series, The Technology Press of The M.I.T. & John Wiley & Sons, Inc., New York, 1950.

4. Kalman, R. E. "On the General Theory of Control Systems", Proc. First IFAC Congress, Moscow, 1960, Butterworths, London, 1961, pp. 481-493.

5. Athans, M. and P. L. Falb. Optimal Control: An Introduction to the Theory and Its Applications, McGraw-Hill, New York, N.Y.

6. Roig, R. W. "A Comparison Between Human Operator and Optimum Linear Controller RMS-Error Performance." IRE Trans. Human Factors Elect., vol. HFE-3, 1962, pp. 18-22.

7. Leonard, T. "Optimizing Linear Dynamics for Human-Operated Systems by Minimizing the Mean-Squared Tracking Error." WESCON, Vol. 4, part 4, 1960, pp. 57-62.

8. Obermayer, R. W. and F. A. Muckler. "On the Inverse Optimal Control Problem in Manual Control Systems", NASA CR-208, 1965.

9. Obermayer, R. W., R. B. Webster and F. A. Muckler. "Studies in Optimal Behavior in Manual Control Systems: The Effect of Four Performance Criteria in Compensatory Rate-Control Tracking", 2nd Annual NASA-University Conference on Manual Control, 1966, pp. 311-324.

10. Miller, D. C. "The Effects of Performance-Scoring Criteria on Compensator Tracking Behavior." Human Factors in Electronics , HFE-6(1), 1965, pp. 62-65.

11. Davenport & Root, Random Signals and Noise, McGraw-Hill, New York, N. Y., 1958, Chapter 8.

APPENDIX

GENERATION OF GAUSSIAN INPUT TAPE

1. Sum of N Uniform Random Numbers

A good approximation to a Gaussian distributed random variable can be obtained by summing a number of uniformly distributed independent random variables. This technique was implemented on the PDP-1 by producing "independent" uniformly distributed pseudo-random numbers by the power residue method described below, then summing these uniform numbers in non-overlapping groups of 31. The approximately Gaussian numbers which resulted were then D-A converted and recorded on analog magnetic tape.

Since the numbers generated by the power residue method have a uniform distribution between +M and -M, they are zero mean. If we perform a scaling operation to simplify the arithmetic, we can equally well imagine these numbers uniformly distributed between -1 and +1.

The first moment (mean) is still zero, the second moment (variance) is now 1/3, and the n^{th} moment is zero for n odd, 1/n+1 for n even.

We will now sum N of these (independent) random numbers and find the moments of the sum:

$$Z = \sum_{k=1}^{N} X_k$$

$$E(Z) = E\left(\sum_{k=1}^{N} X_k\right) = \sum_{k=1}^{N} E(X_k) = \text{ZERO}.$$

$$E(Z^2) = NE(X^2) + N(N-1)\,E^2(X) = NE(X^2) = N/3$$

$$E(Z^3) = NE(X^3) + 3N(N-1)\,E(X)\,E(X^2) + N(N-1)(N-2)\,E^3(X) = \text{ZERO}$$

$$E(Z^4) = NE(X^4) + 4N(N-1)\,E(X)\,E(X^3) + 3N(N-1)\,E^2(X^2)$$

$$+ 6N(N-1)(N-2)\,E^2(X)\,E(X^2) + N(N-1)(N-2)(N-3)\,E^4(X)$$

$$= \frac{N}{5} + \frac{N(N-1)}{3} = \frac{N^2}{3} - \frac{2N}{15}$$

$$E(Z^5) = \text{ZERO}.$$

$$E(Z^6) = NE(X^6) + 15N(N-1)\,E(X^4)\,E(X^2) + 15N(N-1)(N-2)\,E^3(X^2)$$

$$= \frac{5}{9}N^3 - \frac{2}{3}N^2 + \frac{16}{63}N$$

In order to compare these moments with the moments of a Gaussian random number, we should scale Z so that it has unit variance, i.e., define $Z_o = \sqrt{\frac{3}{N}}\, Z$. The n^{th} moment of Z is thus scaled by a factor of $(\frac{3}{N})^{n/2}$:

$$E(Z_o) = 0$$

$$E(Z_o^2) = 1$$

$$E(Z_o^3) = 0$$

$$E(Z_o^4) = 3 - \frac{6}{5N}$$

$$E(Z_o^5) = 0$$

$$E(Z_o^6) = 15 - \frac{18}{N} + \frac{48}{7N^2}$$

If, for example, we choose N = 31,

$E(Z_o)$	$E(Z_o^2)$	$E(Z_o^3)$	$E(Z_o^4)$	$E(Z_o^5)$	$E(Z_o^6)$
0	1	0	2.961	0	14.425

Whereas the normal Gaussian (G) has moments:

$E(G)$	$E(G^2)$	$E(G^3)$	$E(G^4)$	$E(G^5)$	$E(G^6)$
0	1	0	3.0	0	15.0

Thus the sum of 31 uniformly distributed independent random numbers provides a good approximation to the Gaussian distribution. As N is increased, the moments of Z_o converge exactly to those of the Gaussian variable, but the convergence is hyperbolically slow. (Error decreases as 1/N) Increasing N to 62 would only increase $E(Z_o^4)$ to 2.98, so we have probably reached the point of diminishing returns.

2. Generation of Uniformly Distributed Random Variables

The technique used to generate uniformly distributed random variables between the limits +M and -M is described in the IBM publication, "Random Number Generation and Testing." [1/] The suggested procedure involves solving the equation

$$u_{n+1} = (2^{b/2} + 3)\, u_n \pmod{2^b} \qquad (1)$$
$$u_o = 1$$

where $\{u_n\}$ are the values of the random variables with n as an index parameter. b is the bit size of the machine (18 in the case of the PDP-1).

This simple procedure yields a set of uniformly distributed random variables between $-(2^{17} - 1)$ and $+(2^{17} - 1)$ with a period of 2^{16}. Unfortunately this period is much too small. Observe that a random number can be generated by a PDP-1 implementation of equation (1) every 75 μsecs. If these numbers were being generated at highest speed, the series would repeat every $(75 \times 10^{-6}) \times 2^{16} = 4.915$ seconds or about 1/5 cps. This repetition rate is much too fast in view of our goal to generate a signal which looked "white" at low frequencies.

---

1. Random Number Generation and Testing, I.B.M. Reference Manual

Therefore, as an alternative procedure we solved equation (1) setting b = 36. This made the implementation a little more difficult but gave a much longer repetition period. Namely, we used two PDP-1 computer words for u_n. Consider $u\ell_n$ the high order (left half) bits of u_n and ur_n the low order (right half) bits of u_n. Then equation (1) is solved in the following manner:

$$u_n = u\ell_n(2^{18}) + ur_n(2^0)$$

times $(2^{18} + 3)$

---

product $u\ell_n(2^{36}) + 3\ u\ell n(2^{18}) + ur_n(2^{18} + 3)$

Note that we now take this product mod 2^{36} hence:

$$ur_{n+1} = 3\ ur_n \pmod{2^{18}} \qquad (2)$$

$$u\ell_{n+1} = ([3\ ur_n\ (2^{-18})] + ur_n + 3\ u\ell_n) \pmod{2^{18}}$$

where [.] indicates integer part of .

$$u_{n+1} = u\ell_{n+1}\ (2^{18}) + ur_{n+1}\ (2^0)$$

A PDP-1 implementation of equation (2) can generate a random number every 145 μsecs. If these numbers were being generated at highest speed, the series would repeat every $(145 \times 10^{-6}) \times 2^{34}$ = 2,490,000 seconds or a "period" of about 28 days. This is probably sufficient low frequency performance. If the reader is not satisfied with this, he can obviously extend this procedure to any larger value of b with correspondingly slower repetition rates. The actual computer program to implement equation (2) is quite short and is shown below.

called by "jsp random"

$u\ell_{n+1}$ returned in ac

ur_{n+1} returned in io

```
random,         dap r                    *
                law 3
                mul urn
                scr 1s
                dio urn1 /form urn new
                tad urn /urn plus overflow bits of above
                dac t1
                law 3
                mul uℓn
                scl 9s
                scl 8s
                tad t1
                dac uℓn /form uℓn new
                lio urn1
                dio urn
r,              jmp  .
uℓn,            ∅
urn,            1
urn1,           ∅
t1,             ∅
```

Note that bit_r has a period 2^{r-2} hence if only a few bits are to be used from the random number, they should be taken from the high order end of u_n.

---

* a two's complement arithmetic machine is assumed.

3. Content of the Analog Tape

As the Gaussian numbers were generated on the PDP-1, they were D-A converted at a rate of 6 MS/sample and written on the analog magnetic tape at 15"/sec. These samples from a 20-min. record at 15"/sec on track 2 of the tape. On track 1 of the tape is a recording of "zero," which may be used to compensate for errors caused by transport flutter. On track 3 of the tape a $\pm$ 1v control level is recorded which marks those data segments which have been read back (A-D converted) into the PDP-1 and analyzed.

The tape can be played back at any available speed, for instance 1-7/8"/sec, in which case each sample lasts 48 msec and the record is 2 hr. 40 min. in length.

B. ANALYSIS

A 15-second segment of the analog mag tape (about 2500 samples) was read back into the PDP-1 through the A-D converter and the resulting numbers were analyzed to determine how closely they approximated Gaussian "white" samples.

1. Measurement of Central Moments

A program was written to calculate ΣS_k, ΣS_k^2, ΣS_k^3, etc., for the 2500 samples S_k. These numbers were then converted to scaled (unit variance) central moments for comparison with the scaled central moments of a Gaussian distribution. The results were as follows:

	Moment					
	1st	2nd	3rd	4th	5th	6th
SAMPLES	0	1.0	-.05	+3.11	-.3	+14.9
GAUSSIAN	0	1.0	0.0	3.0	0.0	15.0

Thus the first six moments of the samples are in excellent agreement with the Gaussian distribution.

2. High-Frequency Power Spectrum

The autocorrelation function $Rxx(\tau)$ was calculated for shifts τ corresponding to 0, 1, 2, ...25 sample times. The autocorrelation function was assumed to be zero for larger shifts τ, and the Fourier transform of this $Rxx(\tau)$ was taken. This procedure should yield a close approximation to the power spectrum of the samples for high frequencies, but very poor results for low frequencies. If the samples were really "white" (independent) then their power spectrum should be

$$Sxx(f) = \frac{\sin^2 (2\pi f \cdot 6\text{Msec})}{(2\pi f \cdot 6\text{Msec})^2}$$

A plot of both the $\sin^2$ function and the experimentally obtained power spectrum are given in Fig. 1. Note that there is excellent agreement between the two at high frequencies, where the algorithm used was a valid approximation. From this test we may conclude that the power spectrum is that of white samples for high frequencies; we cannot make any statements about the low frequency power spectrum.

3. Low Frequency Power Spectrum

To investigate the spectral power at low frequencies, a set of 100 digital filters were programmed whose impulse responses were sin $2\pi nt/T$ and cos $2\pi nt/T$ where T corresponds to 2500 sample times and n = 1, 2,...100.

The digital filter corresponding to a cos wt impulse response was

$$H_c(Z) = \frac{1 - Z \cos w}{1 - 2Z \cos w + Z^2}$$, where Z represents a unit delay.

The sin wt filter was

$$H_s(Z) = \frac{Z \sin w}{1 - 2Z \cos w + Z^2}$$

Using the sample values as an input to these filters, we see by a simple algebraic manipulation that the outputs of these filters at t = T are the Fourier cosine and sine coefficients, respectively, of the input sample record. Summing the squares of the sine and cosine coefficients of the filters at w provides the amount of power at w. At very low frequencies, this should be constant.

To reduce the large statistical variation of this process, the results were averaged over bands of 1 2/3 cps with the following results:

	0-1 2/3 cps	1 2/3-3 1/3 cps	3 1/3-5 cps	5-6 2/3 cps
Relative power	4.16	5.69	3.69	4.75

The 14% variation in these results is not statistically significant; the standard deviation of this measurement (assuming Gaussian white noise input) is 25% due to the small number of samples. Within the limits of resolution for 2500 sample points, the samples approximate the spectrum of white Gaussian samples down to D.C.

Conclusion

Our analysis of the samples read back from analog tape has verified that the contents of the tape provide a very good approximation to white Gaussian samples: this tape should provide excellent results for anyone whose experiment requires Gaussian white noise.

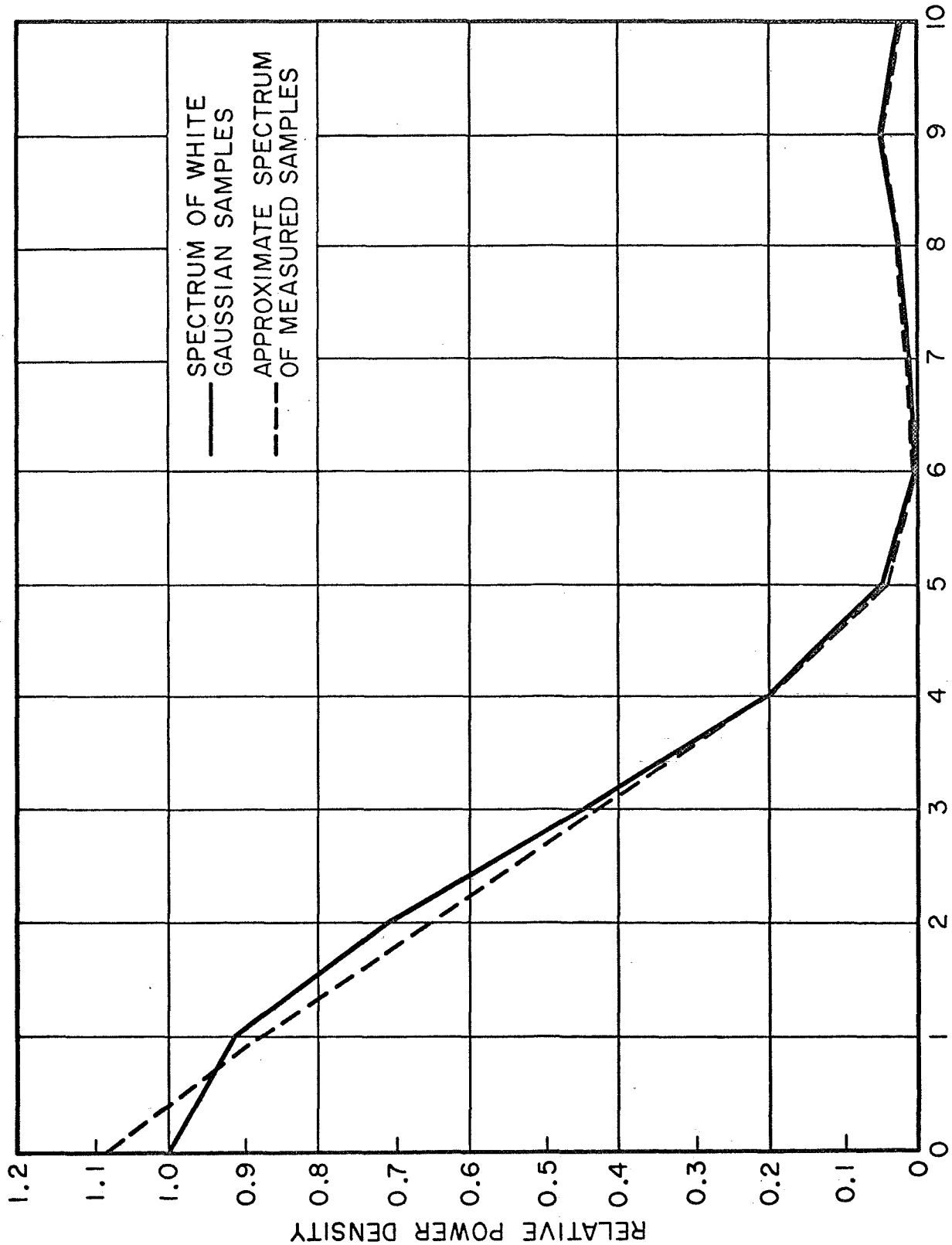

FIG. 1 HI-FREQUENCY POWER SPECTRUM

Unclassified
Security Classification

DOCUMENT CONTROL DATA - R & D

(Security classification of title, body of abstract and indexing annotation must be entered when the overall report is classified)

1. ORIGINATING ACTIVITY *(Corporate author)*
Bolt Beranek and Newman Inc
50 Moulton Street
Cambridge, Massachusetts 02138

2a. REPORT SECURITY CLASSIFICATION
Unclassified

2b. GROUP

3. REPORT TITLE
ON THE OPTIMAL BEHAVIOR OF THE HUMAN CONTROLLER: A PILOT STUDY COMPARING THE HUMAN CONTROLLER WITH OPTIMAL CONTROL MODELS

4. DESCRIPTIVE NOTES *(Type of report and inclusive dates)*
Technical Report

5. AUTHOR(S) *(First name, middle initial, last name)*
Jerry D. Burchfiel
Jerome I. Elkind
Duncan C. Miller

6. REPORT DATE	7a. TOTAL NO. OF PAGES	7b. NO. OF REFS
15 August 1967	63	11

8a. CONTRACT OR GRANT NO.	9a. ORIGINATOR'S REPORT NUMBER(S)
NAS12-104 b. PROJECT NO.	BBN REPORT NO. 1532
c.	9b. OTHER REPORT NO(S) *(Any other numbers that may be assigned this report)*
d.	none

10. DISTRIBUTION STATEMENT
Distribution of this document is unlimited.

11. SUPPLEMENTARY NOTES	12. SPONSORING MILITARY ACTIVITY
none	NASA, Control and Information Systems, Electronics Research Center, Cambridge, Massachusetts 02139

13. ABSTRACT

It is postulated that the human controller acts in a near optimal manner given his inherent structural constraints. These constraints are approximated by a time delay. The optimal controller for a linear plant with a quadratic cost functional which takes into account this time delay limitation is derived. The optimal controller contains a model of the plant being controlled plus linear dynamics operating on the difference between the output of the real plant and that of the model. A pilot experiment was performed to test the hypothesis that the human controller is nearly optimal. Good agreement between human and optimal controller behavior was obtained. The differences between the two behaviors can be accounted for by assuming a subjective cost functional that the human controller attempts to optimize.

DD FORM 1 NOV 65 1473 (PAGE 1)
S/N 0101-807-6811

Unclassified
Security Classification

14. KEY WORDS	LINK A		LINK B		LINK C	
	ROLE	WT	ROLE	WT	ROLE	WT
Manual control						
Optimal control						
Tracking						
Human operators						